University of Southern Indiana
Pott College of Science, Engineering, and Education
Engineering Department
8600 University Boulevard
Evansville, Indiana 47712

Characterizing a Quantum Cascade Meta-Surface Amplifier at Terahertz Frequencies

Kassidon Hatfield
Briston Bundy

ME491 – Senior Design Fall 2023

ACKNOWLEDGEMENTS

We would like to thank our senior design faculty advisor, Dr. Jenna Kloosterman, for not only being an immense help during both semesters of this project, but also traveling to JPL with us, and being a wonderful mentor. Also, we would like to thank Dr. Kissel for sharing his love of optics with us and helping us organize our project during its beginning stages. We would also like to thank Justin Amos for manufacturing the optics for us. For traveling with us and being a part of this project along the way we would we like to thank Melanie Cedeno, Derrick Thompson, Miguel Pinto, and Jimmy Hunnicut. Finally, we would like to thank Dr. John Kawamura, Dr. Chris Curwen, Dr. Jose Siles.

ABSTRACT

The objective of this project is to measure amplification from a terahertz quantum cascade metasurface amplifier. In this project an optical testbed was designed to accomplish this objective. This will aid in the study of Giant Molecular Clouds (GMCs). GMCs have been an area of great interest for astronomers and the current technology being used for this, the THz heterodyne receiver, could be improved using an amplifier in the signal path between the sky and the mixer as is done for lower frequency heterodyne receivers. Although other projects have demonstrated amplifiers based on quantum cascade gain materials, they could not be implemented into heterodyne receivers because their output signals could not be coupled to the next element in the receiver chain. A recently designed amplifier at the Jet Propulsion Laboratory uses a quantum cascade metasurface in place of the previously used waveguide structure that can overcome this challenge. To design the optical test bed, a mirror block was designed to focus light from the source to the meta-surface and subsequently focus the amplified light from the meta-surface onto a detector. This mirror block and the testbed had their geometry, structure, and placement calculated using a python script written for that purpose. This design was simulated in SolidWorks to make sure the components would all fit in the area allotted. The resulting testbed design achieved an angle of incidence of 5.08 degrees and a theoretical beam radius of 0.3993 mm and a beam diameter of 0.7986 mm at the metasurface. The design met the requirements, and the design was tested at JPL in June. The experimental beam diameter was 1.2 mm; however, we measured an amplification of 6 dB at 2.48 THz. We consider this a success, but future projects will try to reduce the beam size to fit the original requirement.

Table of Contents

List of Figures

List Of Tables

List of symbols

Symbol	Description
E	Energy level difference
h	Placnk’s constant
υ	Frequency of Radiation
E_{high}	Atoms at a higher energy level
E_{low}	Atoms at a lower energy level
ω_0	Beam Waist
λ	Wavelength
c	Speed of Light
f_1	Focal Length 1
f_2	Focal Length 2
C	Distance between focal lengths
a	Semi-major axis of ellipse
b	Semi-minor axis of ellipse
M	Magnification
ω_{out}	The beam waist coming out of the mirror
ω_{in}	The beam waist coming into the mirror
Z_1	Distance from mirror to detector or source
Z_2	Distance from mirror to meta-surface
ω_z	Beam radius at some distance Z

1. Introduction

A quantum cascade metasurface amplifier (QCMSA) is a patch antenna, which is an antenna with a low-profile and a periodic structure, filled with quantum cascade gain material. This gain material can be described as layers of semi-conductors specifically layered so electrons cascade down the material and emit photons at a specific wavelength related to the energy lost in that cascade. The Jet Propulsion Laboratory (JPL) has designed a QCMSA to potentially increase our ability to probe the interstellar medium (ISM), the gas and dust that fills the space between stars. Part of the ISM consists of giant molecular clouds (GMCs), which provide environments in which new stars form and can be probed in the Terahertz region of the electromagnetic spectrum. JPL, a federally funded research laboratory ([1]), asked us to design an optical testbed that would measure the amplification of the QCMSA at terahertz (THz) frequencies and then perform those measurements at JPL. THz frequencies of light have wavelengths shorter than microwave, but longer than infrared.

1.1 Objective

The objective of the project is:

To measure amplification from a terahertz quantum cascade meta surface amplifier.

1.2 Deliverables

The deliverables for this project are:

- A design of an experiment including optics showing amplification from the quantum cascade metasurface amplifier.
- A senior design report that includes a summary of the results.
- A presentation of the project.
- A poster explaining the project.

This report will further cover the background and describe similar projects in the next section. It should be noted that this is a new and novel amplifier at the cutting edge of technology research and as such there are not many projects that are like ours. Subsequently, the literature discussed is similar, but not exactly identical to parts of our project. Moving on, there will be a discussion of the designs that were looked at during this semester followed by an in-depth explanation and analysis of the design chosen, its implementation at JPL, and the measurements it enabled. Finally, there will be a conclusion to wrap things up.

2. Background

2.1 Statement of the Problem

Stars are created from GMCs mostly made of gas with a smaller amount of dust. The dust particles mostly consist of carbon and silicon and the gas consists mostly of molecular hydrogen with trace amounts of oxygen and nitrogen ([2]). The density of a cloud's core, which is made up mostly of hydrogen, increases as this cloud accumulates mass. As the cloud's core condenses, the cloud begins to release the thermal energy in the core by emission through the THz fine structure lines of [C II], [N II] ([3]), and [O I] ([4]).

These atomic tracers offer a convenient way for astronomers to study conditions in the ISM. Astronomers utilize the heterodyne receiver, which is commonplace in radios and wireless communications at lower frequencies, to measure the spectral lines from these elements by mixing the sky signal with a lab generated local oscillator ([4]). The heterodyne receiver works by combing the local oscillator frequency and the received frequency to produce a "beat" frequency, which is the difference between the two frequencies ([5]). At frequencies that can detect [CII], [NII], and [OI] fine structure lines, the resulting mixed signal is usable, but there is a large amount of noise that reaches the mixer, so longer observational times are required to achieve a good signal-to-noise ratio.

This noise can be reduced or eliminated by adding an amplifier in the path between the mixer and the sky signal as is done in lower frequency radios; However, no suitable amplifier existed at the target frequencies until the Jet Propulsion Laboratory (JPL) demonstrated one last year based on a quantum cascade meta surface (QCMS). Our project is to design an optical testbed to characterize and optimize the amplification from the second generation QCMS amplifier hereafter referred to as the QCMSA. A QCMSA is like a patch antenna, a low-profile antenna that can be mounted on a surface ([6]), made from an array of periodic waveguides consisting of with quantum cascade gain material and is like a quantum cascade laser (QCL) in behavior except that radiation is amplified and reflected rather than created by a population inversion. Amplification of optical signals is based on quantum mechanics. An atom's electrons occupy distinct energy levels that they can travel between by absorbing or emitting photons at a frequency found in Equation 1:

$$E = h\upsilon \quad (1)$$

Where "E" is the difference in energy between the two levels, "h" is Planck's constant, and "υ" is the frequency of the radiation. Now if there was a collection of atoms, a majority of which were in a higher energy level (E_{high}) and a minority of which were in lower energy level (E_{low}), and a photon at a frequency of $\upsilon = \frac{E_{high} - E_{low}}{h}$ passes through this collection of atoms, more electrons will go from E_{high} to E_{low} than the other way around. This means that when a certain number of photons come in, more come out, which means the light has been amplified. This condition, having more electrons in E_{high} than E_{low}, is referred to as a population inversion. We achieve this state in a QCMSA by driving a bias voltage through the quantum cascade gain material. This bias voltage which acts as a starting kick and drives the electrons into a higher energy state within the valence band. However, this quantum cascade gain material can only be produced in very small quantities, meaning we cannot just make a large block of it and send a THz beam through it like we are planning with the meta surface. Instead, we use metallic antennas and waveguides to collect the THz radiation, concentrate it in the amplifying material, and then re-radiate it back to free-space ([7]) ([9]).

JPL used the QCMSA to demonstrate amplification of a CH_2F_2 far-infrared gas laser operating at 2.743 THz (109 µm), but their first effort achieved only 0.3 dB amplification. They are currently working to improve the design and increase the gain by optimizing the thickness and shape of the metasurface and raising the order of the transverse resonance [9]. Resonance in terms of light, is the interaction of electromagnetic waves with materials at specific frequencies, leading to the enhancement or absorption of light. The transverse resonance in the metasurface is a phenomenon where the magnetic and electric fields are coupled to the elements within the metasurface. That coupling leads to a resonance within the metasurface. However, these resonances are transverse, meaning that they occur perpendicular to the direction of the incident light. If our project is successful, the QCMSA will be tested in a heterodyne receiver to improve the sensitivity of heterodyne receivers and, in turn, be one step closer to achieving a higher signal to noise that would allow THz astronomers to learn much more about GMCs. The heterodyne receiver tests will be left to a future senior design project for current USI juniors.

2.2 Similar projects

2.2.1 Measurement of Amplification and Absorption of a THz Quantum-Cascade Meta-Surface free-space Amplifier

The closest project to ours would be the previously mentioned experimental design shown in Figure 1 by a group at JPL [8].

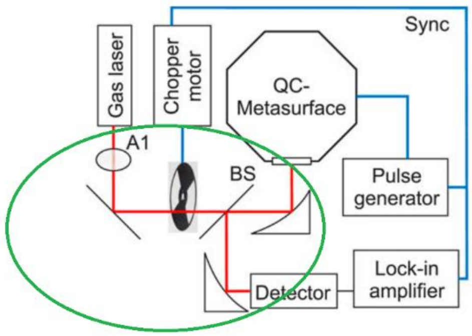

Figure 1. This figure shows the experimental setup of a QCMSA test at JPL ([10]). The optics to be designed as part of our senior design project are circled in green. Since we are using a different source with significantly less power, there will be significant changes to the optical testbed.

The QCMSA is made of an array of metal-to-metal ridge waveguides loaded with quantum cascade gain material and has been demonstrated to be able to successfully amplify a CH_2F_2 far-infrared gas laser operating at 2.743 THz as shown in the green band of Figure 2([10]).

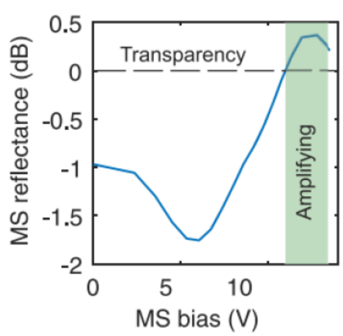

Figure 2. Measured Meta-Surface reflectance as a function of bias voltage ([10])

In the setup, the laser source is optically chopped at 100 Hz, the metasurface bias was synchronized with this chopping ([10]). As reported, this setup is not optimal for amplification ([10]). The group also used ridge waveguide arrays, which could be improved.

2.2.2 X-ray microfocusing with off-axis ellipsoidal mirror

A group from Japan Synchrotron Radiation Research Institute designed an off-axis elliptical mirror so they could develop improved fabrication techniques for ellipsoidal focusing mirrors in the hard-X-ray region ([11]). Their elliptical mirror shown in Figure 3 had two focal lengths, focal lengths will be more deeply discussed in a later section, one was fifty meters and the other of a fifth of a meter.

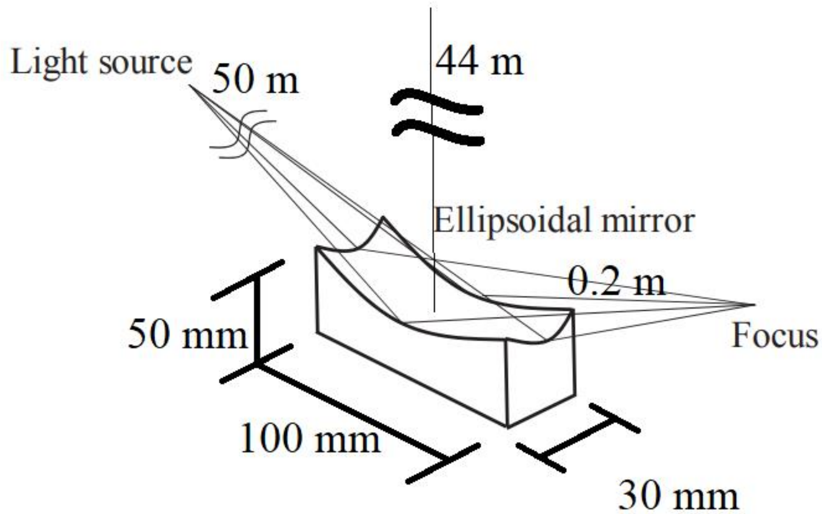

Figure 3. Schematic of off-axis ellipsoidal focusing mirror ([11])

The mirror also had a substrate, the surface that the mirror coating was deposited on, of 100 mm and a radius of curvature of 44 m along the long-axis direction. First the ellipsoidal shape was fabricated using precision grinding with a surface figure accuracy of several hundred nanometers height before the surface roughness was reduced to and surface roughness was reduced to 0.2 nm Root Mean Square (RMS) ([11]). Next, the surface was finished by using a computer-controlled figure correction process ([11]).

2.2.3 Single mode terahertz quantum cascade amplifier

Cavendish Laboratory, University of Cambridge, produced an amplifier that used a 2.9 terahertz quantum cascade laser ([12]), the setup for which is shown in Figure 4. They deposited an antireflective coating on the Quantum Cascade Laser (QCL) facet which in turn suppressed the lasing action ([12]). Suppressing the lasing action this way allowed QCL to be used as an amplifier ([12]). The amplifier had a maximum optical gain of 30 dB with a high signal to noise ratio. On top of this, the power consumption was small ([12]).

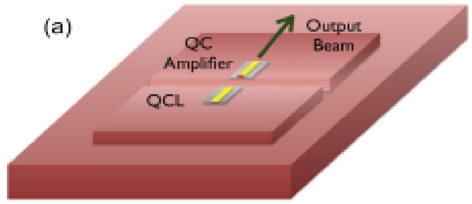

Figure 4. Schematic drawing of the measurement setup

2.2.4 What Learned

Based on the experiment conducted at JPL in 2022 ([10]) we set the amplification level that would make the next generation QCMSA technology a success. This paper also informed us that we will probably need to adjust the voltage bias to maximize the amplification during testing.

From the experiment conducted at Japan Synchrotron Radiation Research Institute, we learned a good amount of information about elliptical mirrors, which has been critical for our design. Firstly, it helped familiarize us with some of the terminology associated with elliptical mirrors and mirrors in general such as substrate, the surface that the mirror coating was deposited on, and focal length, the lengths at which if light passes through one focal length, it must pass through the other. This also made us aware of the difficulty associated with the production of mirrors. This helped in determining the timeline necessary to manufacture the mirror.

We got a better understanding of a non-metasurface QCL from the experiment at Cavendish Laboratory. The lead to a better understanding of the metasurface as a whole and facilitated the explanation that was given earlier in this report. It also helped us understand the reasons that a traditional non-metasurface QCL that did not couple well to free space [7]. For use in a heterodyne receiver, the amplifier will need to have a good coupling to free space to ensure signal reaches the mixer, which is the next component in a heterodyne receiver chain.

2.3 Requirements

Table 1. Requirements

1. The diameter of the mirror shall be at least 2 times the size of the beam radius, which is dependent on frequency
2. The angle of incidence between the metasurface and beam shall be between 5-10 degrees

4. The meta surface shall be placed at least 5 mm away from the cryostat window
5. The window on the QCMSA cryostat shall be at least three times the beam radius
6. The experiment shall measure an amplification that exceeds 0.3 dB
7. The sizing of the optics shall be compatible with a source beam waist of 0.242 mm
8. The beam diameter at the metasurface shall remain under 1 mm

3. Initial Conceptual Designs

3.1 Design Considerations

This project did not design the metasurface, which requires a background in patch antennas and QCLs. Instead, this project aims to design the optics and experiment needed to measure the amplification of the Quantum Cascade Meta-Surface Amplifier (QCMSA). The main detail needed to do this project is that the meta-surface will reflect amplified light into free space. In other words, it will act as a flat mirror reflecting a source of light at its angle of incidence and the amplification occurs because a bias voltage is applied across the surface. This bias voltage will be determined though experimentation.

For our design we need to focus the beam coming from the source onto metasurface at different frequencies. On top of this, the more optical elements we add, the more amplification will be lost. With this in mind, we want a design that focuses light from one place to another, has consistent behaviors between different frequencies, and minimizes the number of optical elements used. It would also aid in experimental setup if the design could be aligned with a visible red laser, so making the design function with visible light would be helpful.

With these considerations in mind, we settled on using at least two elliptical mirrors. These mirrors allow us to easily focus light from one place to the next because any light going through one focal point of the mirror must go through the other focal point of the mirror ([8]). On top of this, when components, such as the source and metasurface, are placed at these focal points, changes in frequency do not change the distances required between the components. This non-frequency-dependent behavior can be replicated with lenses, but it takes two lenses instead of one mirror to achieve said non-frequency dependence. To allow for red laser alignment, we also decided the mirrors should be polished to visible light quality. One of the disadvangtes of elliptical mirrors is, the manufacturing process for elliptical mirrors can be costly and lengthy, and most manufacturing companies will only work with businesses or the government. However, we are still confident that elliptical mirrors are the right choice.

3.2 Concepts

3.2.1 Single Mirror Mounted on Optical Table

The single elliptical mirror mounted onto the table required only one mirror that would have to be manufactured shown below in Figure 5. While this did pose the problem of finding a manufacturer, the ability to hand tailor the focal lengths, move it around on the table, and place it further from the cryostat made us go with this design over the next two designs.

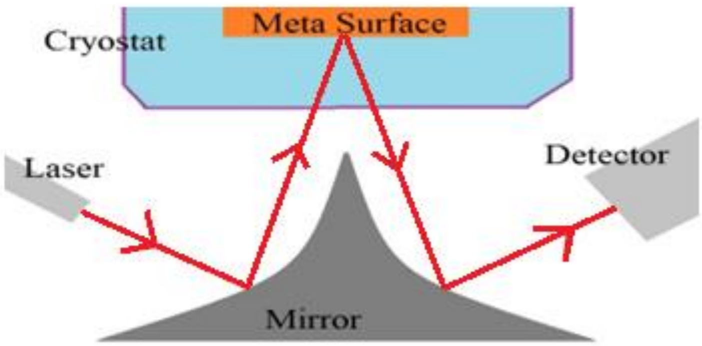

Figure 5. 1st Conceptual Design

3.2.2 Two Stock Mirrors Mounted on Optical Table

This conceptual design consisted of two separate mirrors that would be purchased shown in Figure 6 below. These mirrors would be mounted on the optical table with mounts either designed or purchased. The mirrors that would be purchased provided a limited number of focal lengths, which restricted many design aspects. The limited number of mirrors online did end up becoming a problem once the design progressed.

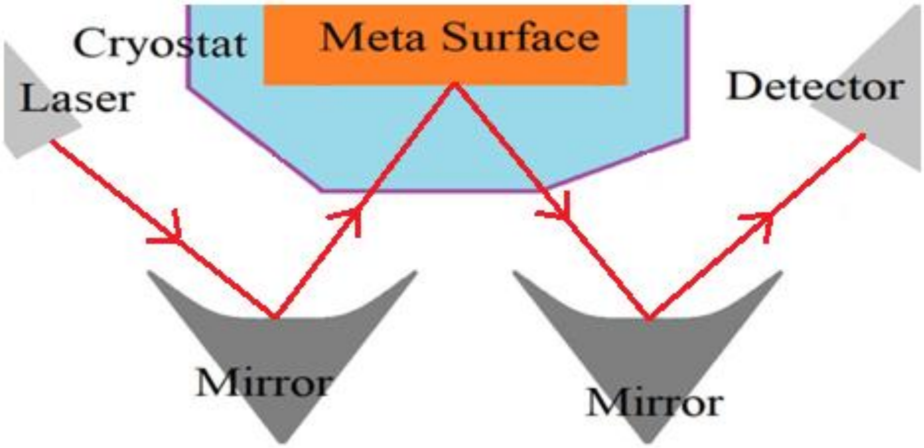

Figure 6. 2nd Conceptual Design

3.2.3 Single Mirror Mounted onto the Cryostat

The final conceptual design, shown in Figure 7 below, consisted of a single designed mirror that would be mounted on the cryostat. This design would allow for easy micro adjustments with the design of our choice. However, it ended up not being a very practical design, and this was due to JPL informing the team that the mirror wouldn't be able to get that close to the cryostat.

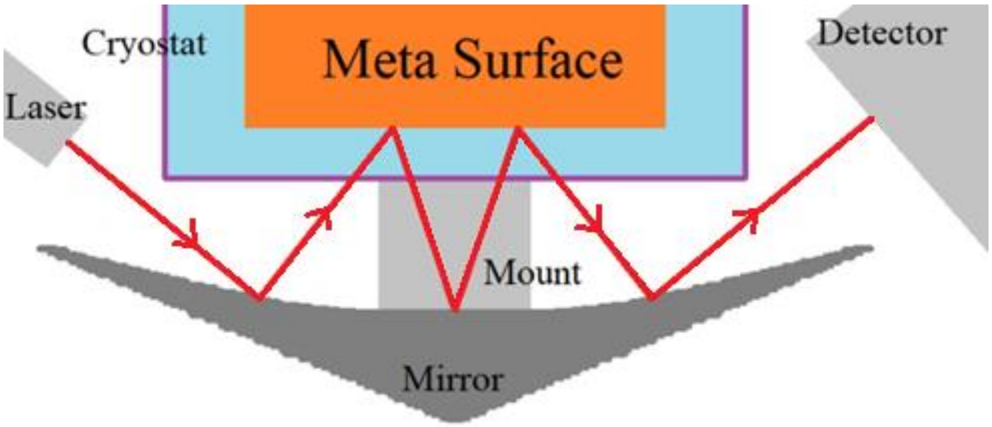

Figure 7. 3rd Conceptual Design

3.3 Pros and Cons of each Conceptual Design

Table 2.Pros and Cons of Conceptual Designs

	Pros	Cons
Design 1	• Easier to micro adjust • Can be tailored to our requirements	• More costly • More intensive design • Difficult to have made
Design 2	• Better cost • Less intensive design	• Not easy to adjust • Cannot be tailored to our requirements • Limited by what is in stock online
Design 3	• Simpler mirror design • Easy to adjust	• Cost • Design not feasible for our needs • Difficult to have made

4. Final Engineering Design

4.1 The Design

The final design for this project was a single mirror that mounted on the optical table shown in Figure 8. A concept of operations is shown in Appendix B and a mechanical block diagram is shown in Appendix D. This design was chosen because the stock mirrors available online could not fulfill the requirements and the mount to the cryostat design proved wholly impractical. After each component, or a representative component, was designed, it was slotted together in solid works to see if it all would fit together.

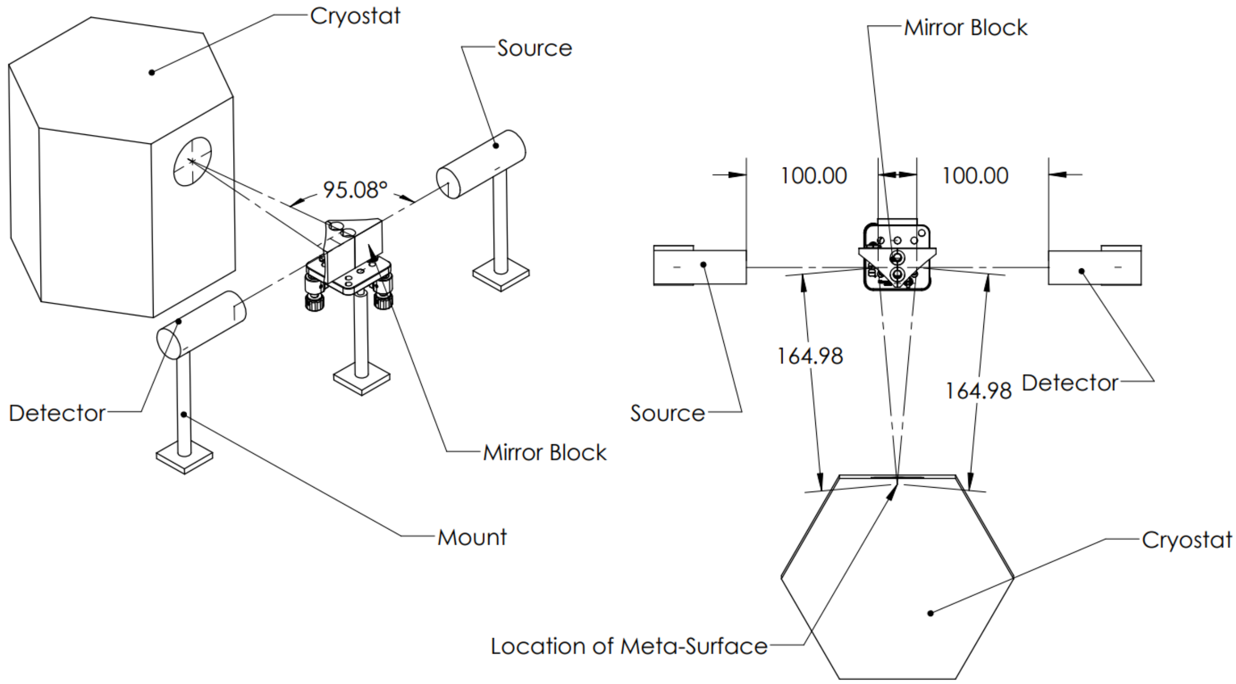

Figure 8. The final optical testbed setup. (Note: some of the components that were provided by JPL do not look like their real-life counter parts in this design. This is because we were not provided with photos of said components)

4.2 Some of the materials provided by JPL

To start off the optical design, the Jet Propulsion Laboratory (JPL) has provided some initial values about the optical parameters of the source to be amplified. These are shown in Table 3.

Table 3. Given Values

Beam waist out of the Feed Horns (ω_0) (see Figure 10)	0.242 mm
Frequency of Source (υ)	2.7 THz (1 THz= 1 x 10^{12} Hz)

The source is a 2.5-2.7 THz frequency multiplier chain (FMC) shown in Figure 9, which employs non-linear diodes to create harmonics until the desired frequency is reached. It emits electromagnetic radiation in the frequency range of 2.5-2.7 THz and was developed at JPL for a different project that is no longer using it.

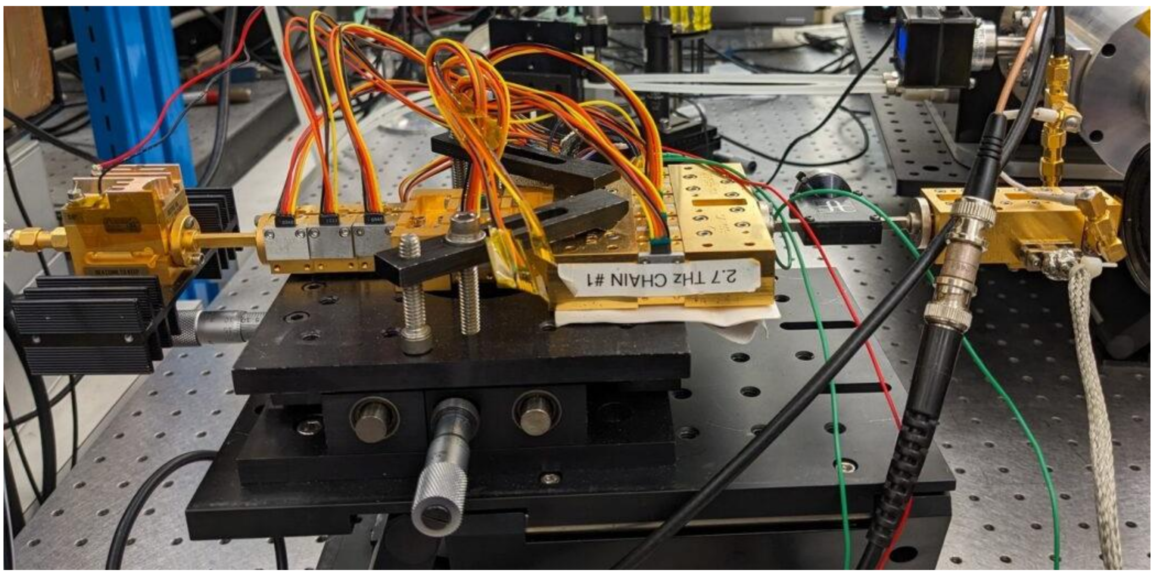

Figure 9. 2.5-2.7 THz Frequency Multiplier Chain (FMC)

The source has a diagonal feedhorn with a beam waist of 0.242 mm. The beam waist, as shown in Figure 10, is the radius of a Gaussian electromagnetic beam at its smallest diameter. Unlike optical wavelengths, where ray tracing is an acceptable method of optical design, beam radii in the terahertz regime are too large to be ignored ([13]).

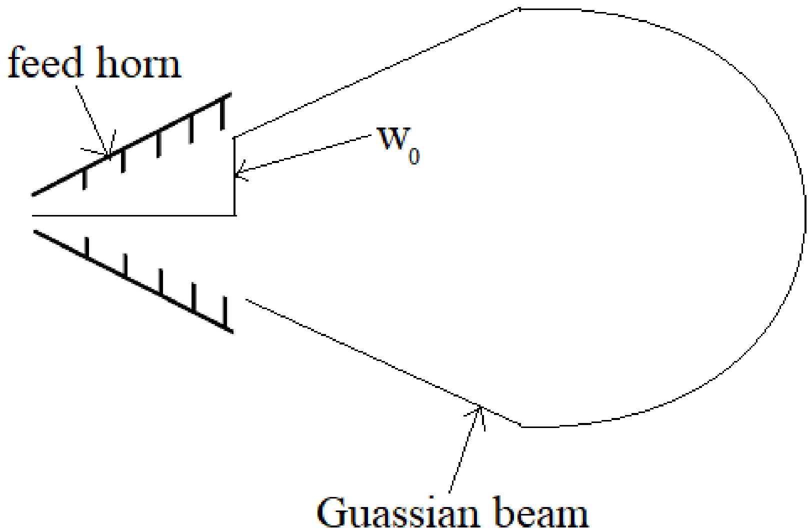

Figure 10. A diagram showing the beam waist as it comes out of the feed horn.

Diagonal feed horns are popular because of their low sidelobe levels and low cross-polarization effects. A feedhorn, in this case, is cone like antenna ([13]). Corrugation helps to lower the sidelobes and cross-polarization of the feedhorn ([14]). For our application, the lower sidelobes levels and cross-polarization are important to couple more power to the QCMSA.

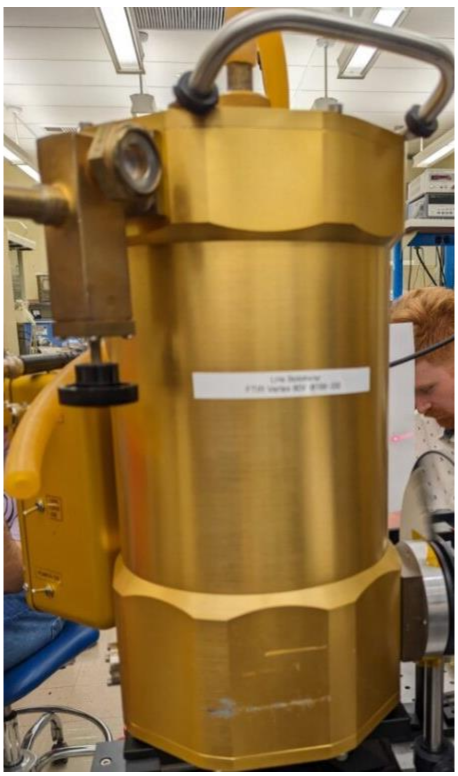

Figure 11. The liquid helium cryostat housing a silicon bolometer.

The detector, a silicon bolometer, is shown in Figure 11, and will be provided by JPL as well. The bolometer measures the change in light, so it will be paired with a chopper wheel shown in Figure 12. The chopper wheel modulates the incoming signal between and on and off position at a set frequency, so the bolometer detects the difference between the THz radiation beam and its background.

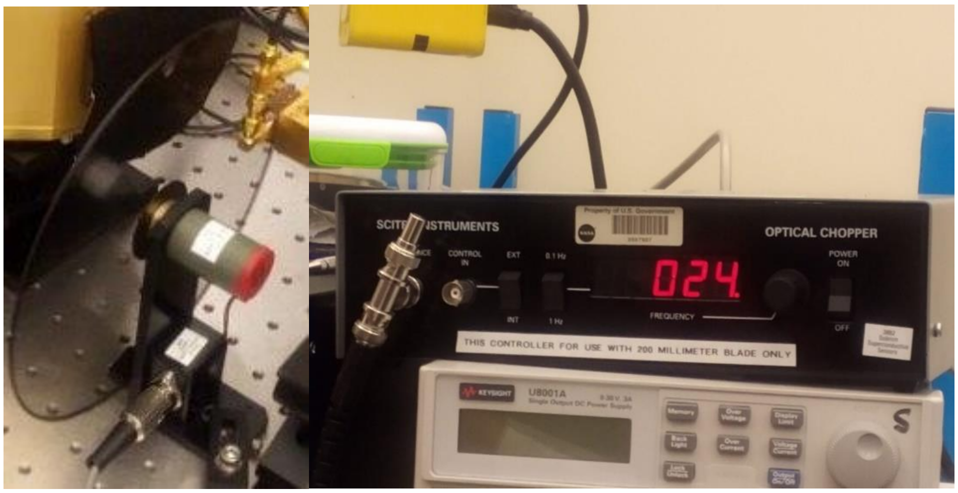

Figure 12. Chopper and its frequency controls

Quantum cascade metasurfaces (QCMS) require cooling to at least liquid nitrogen temperatures (77 K) for operation. This cooling power will be provided by a Stirling cooler and a temperature control loop will adjust the power necessary to maintain the QCMSA at a constant bath temperature. We were assured by JPL that the Stirling cooler, shown in Figure 13, will be able to remove the heat load from the metasurface.

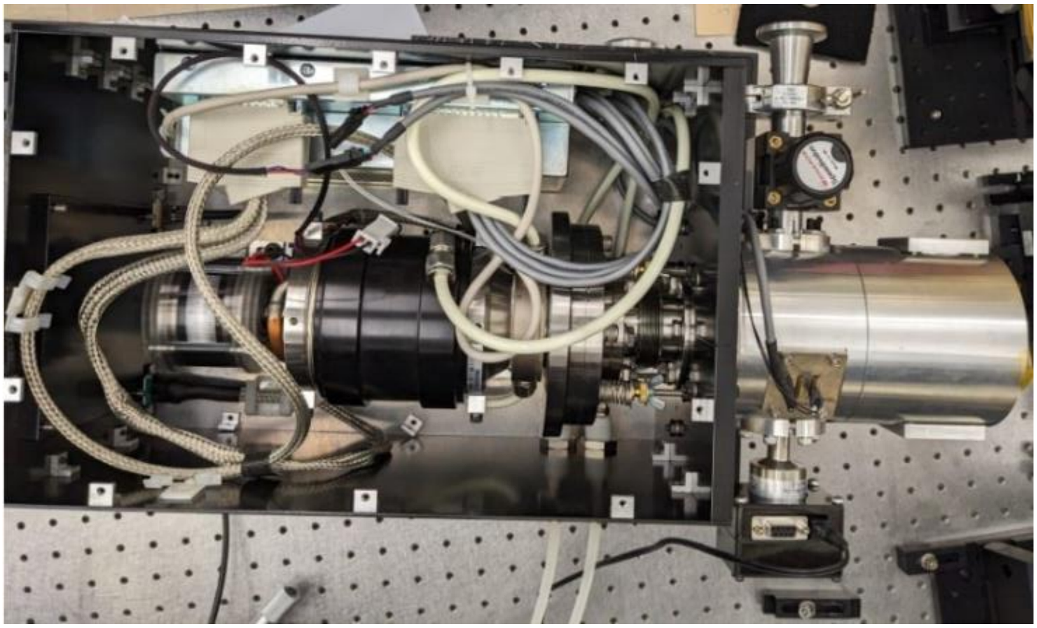

Figure 13. The Cryostat from The Top

4.3 The ellipsoidal mirror

The material used for the mirror does not have any requirements, so we will use aluminum to keep down costs. We will use an offset axis, ellipsoidal mirror shown in with a 100 mm focal length 1 (F_1), a 160 mm focal length 2 (F_2), and a 29.21 mm diameter for each side (see Figure 14 below).

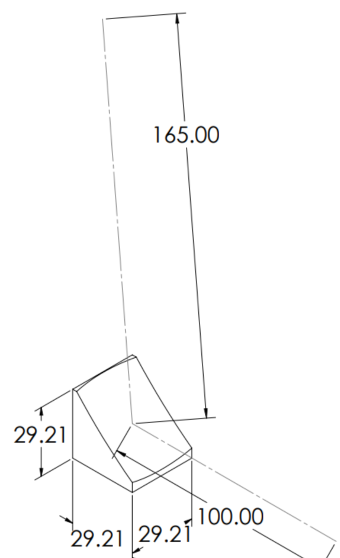

Figure 14.One Side of The Ellipsoidal Mirror

This means the curvature of the mirror is that of part of an ellipsoid, the three-dimensional shape based on a two-dimensional ellipse, with the focal lengths being the distance from the mirror to the focal points of the ellipsoid where the angle between the two distances is the offset angle ([8]) ([15]) ([16]). A reference to an ellipse and some common distances can be seen below in Figure 15.

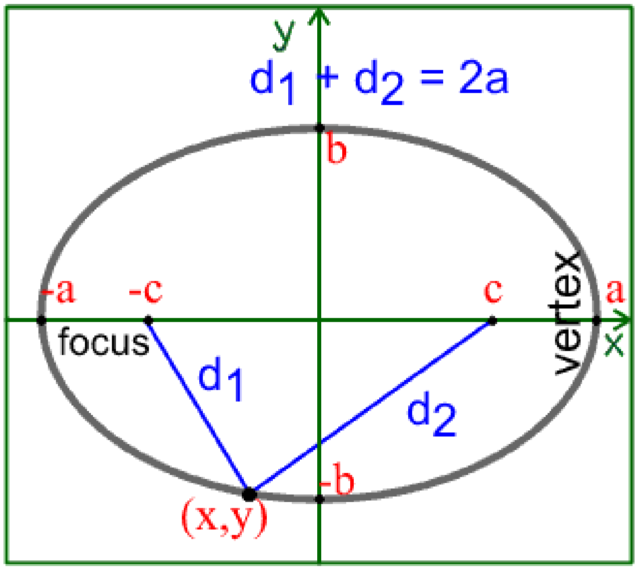

Figure 15. An Ellipse and Some Common Distances Associated with It

This figure will be helpful as these distances are shared between an ellipse and an ellipsoid. All the calculations done were done with a python script shown in Appendix E. To get the distance between the focal points, the offset angle was set to ninety-five degrees. This meant that the two focal lengths and the distance between the two focal points made up a triangle with the distance between the two focal points being the third leg of said triangle. This information, the law of cosines, and the definition of an ellipse ([16]) lead to the definition of Equation 3:

$$(2C)^2 = \sqrt{(\,(f_1\,)^2 + (f_2\,)^2 - 2 * \; f_1 * f_2 * \cos(95))} \rightarrow 2C = 200.25\, mm \tag{3}$$

The following equations, Equation 4, Equation 5, and Equation 6 were used to derive the geometry of the ellipsoid needed and the magnification of the mirror:

$$a = \frac{f_1+f_2}{2} = 132.5\, mm \tag{4}$$

$$b = \sqrt{(a^2 - C^2)} = 86.7811\, mm \tag{5}$$

$$M = \frac{f_2}{f_1} = 1.65 \tag{6}$$

All this information comes together to give us the ellipse shown in Figure 16 and info shown in Table 4:

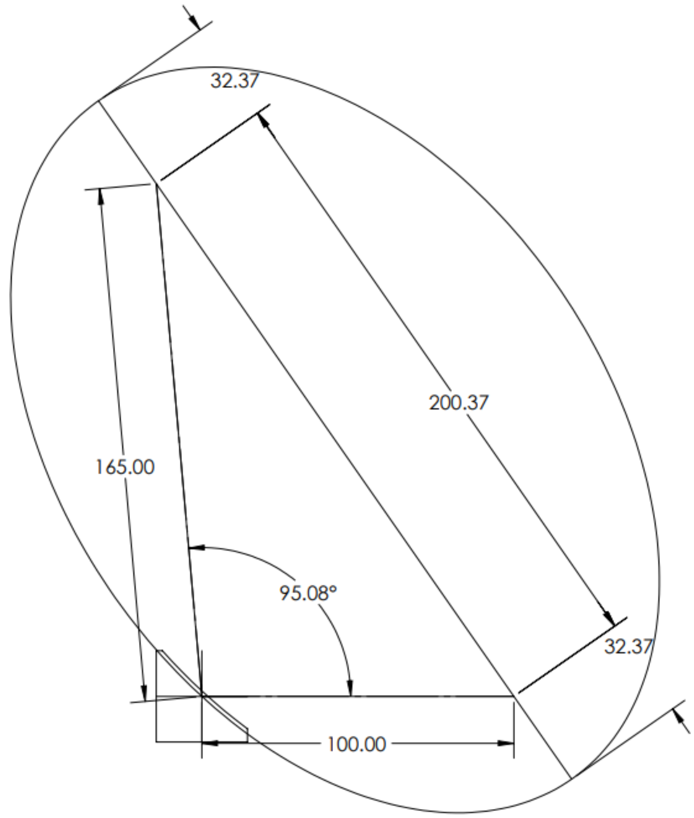

Figure 16. The Base Ellipse (Note: the Solidworks drawing's dimension are slightly off)

Table 4. The dimensions and data of the ellipse

Distance from one focal point to center of ellipse (C)	100.185 mm
Semi-major axis of the ellipse (a)	132.5 mm
Semi-minor axis of the ellipse (b)	86.78 mm
The length of the triangle formed by the two focal lengths (2*C)	200.37 mm
The Angle between the two focal lengths	95.08°
Focal Length 1 (f_1)	100 mm
Focal Length 2 (f_2)	165 mm
Magnification (M)	1.65

With all of these in place we can find the curvature of the mirror. Below is Figure 17, a picture of one side of the custom mirror based on the ellipsoid also pictured in Figure 17.

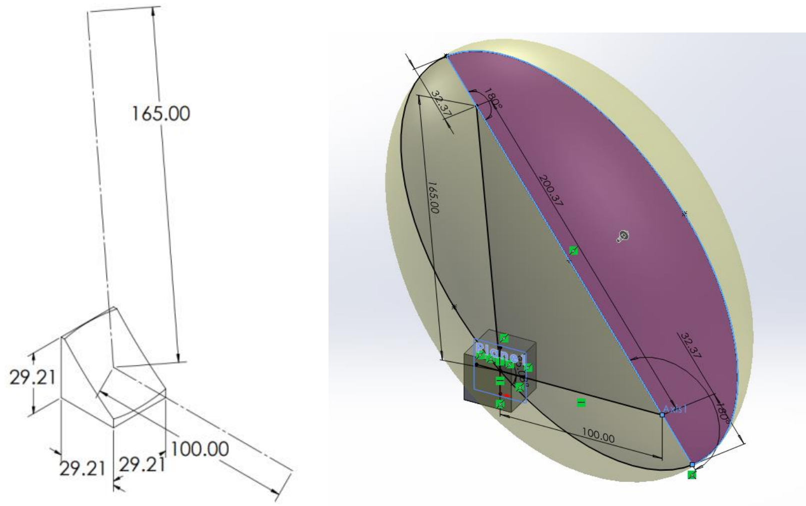

Figure 17. One Side of The Ellipsoidal Mirror and the Ellipsoid That Defines Its Curvature

The main reason for using an ellipsoidal mirror is that when light comes from one focal point, it must pass through the other focal point ([8]). This means that if the feed horn is placed at one focal point, all the light from the feed horn must pass through the other focal point. This means we can place the metasurface at the other focal point and know that the beam will be focused down to a beam waist given by Equation 7:

$$\omega_{out} = M * \omega_{oin} = 0.3993\ mm \tag{7}$$

The beam diameter at the meta-surface is ω_{out} times 2, which here equals 0.7986 mm. This meets our requirement for the beam diameter at the metasurface. This of course means the distance from the mirror to the feed horn (Z_1) will have to be equal to F_1 and the distance from the mirror to the meta-surface (Z_2) will have to be equal F_2 to achieve this behavior. JPL requested that the beam waist at the metasurface be at least $2\omega_{oin}$ which the current setup more than achieves. Another reason an ellipsoidal mirror was used was due to the offset axis. The offset axis is necessary because JPL informed us that the source and detector would not fit next to the cryostat, which meant we need a way to change the direction of the beam to allow for space between the components. This mirror needs to have a diameter that is at least 2 times the size of the beam when it reaches the mirror (ω_z) to prevent any light from escaping. We find ω_z using Equation 8 ([14]):

$$\omega_z = \sqrt{{\omega_0}^2 * \left[1 + (\frac{\lambda z_1}{\pi {w_o}^2})^2\right]} = \sqrt{(0.000242)^2 * \left[1 + \frac{(0.0001110342)(0.1)^2}{\pi(0.000242)^2}\right]} = 14.6\ mm \qquad (8)$$

If we take 14.6 mm and multiply it by 2, we get 29.2 mm. The effective diameter of the mirror is the side that the beam is nearly perpendicular to in this case. 29.2 mm is smaller than the effective diameter of our chosen mirrors, the mirror is suitable for our purposes. One of the requirements we are under is that the window on the QCMSA cryostat needs to be at least three times the beam radius. In this case the window is 4 cm in diameter, meaning the beam needs to be under 13.33 mm.

Figure 18. The QCMSA is located just behind the TPX window of the Stirling Cooler. This window is transparent at THz frequencies and acts as filter to reduce the heat load on the Stirling cooler due to the external environment.

To determine the beam radius at this position, we will use Equation 8, but act as if the beam is coming from where the metasurface is placed (meaning we set Z_1 to the distance from the meta-surface to the cryostat window), which is 5 mm (see Figure 8), and we replace ω_{0in} with ω_{0out}. We multiply this beam radius by two, this will give us a beam diameter of 1.1921 mm, which easily meets the requirement. On the other side of the mirror block assembly will be a mirror of identical curvature. We can do this because the metasurface behaves as a flat mirror, meaning the angle of incidence is equal to the angle of reflection. This means we can place our identical mirror with its F_2 receiving the beam coming from the meta-surface and place the detector's feed horn at the F_1, causing it to have the same beam radius as at the first feedhorn. The detector feedhorns can be over-moded, so they will accept the same beam waist. Using this data, the final mirror block designed is shown in Figure 19.

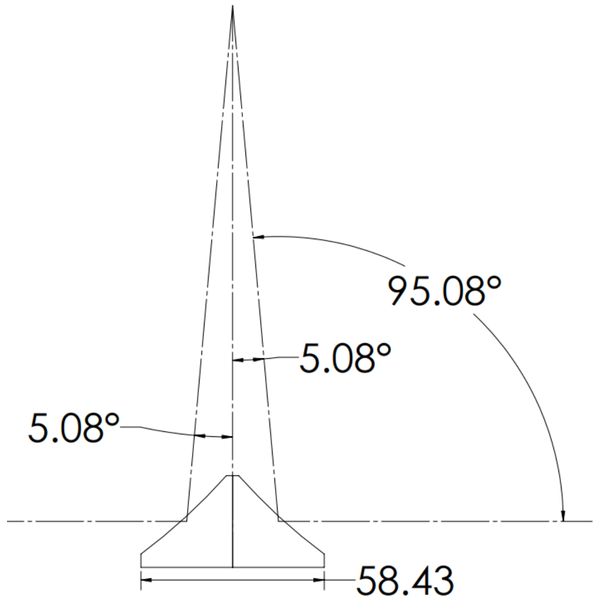

Figure 19. The final elliptical mirror block design used in our testbed

The 5.08° shown in Figure 19 is the angle of incidence between the beam and the metasurface and fulfills the requirement that the angle of incidents to the metasurface be between five and ten degrees. The lower limit on this requirement is to prevent the incoming beam and outgoing beam from interfering with each other. The upper limit is to prevent the metasurface from acting like a diffraction grating to the incoming beam. Using an offset angle of 95° meant the geometry would allow the back sides of the mirror block to be parallel against one another as shown above in Figure 19.

4.4 Mountings

The cryostat, detector, and the source will come with their own mounting mechanisms provided by JPL. The mirror block will be mounted via 5.11 mm diameter screws that will go into the holes on the top of the mirror block and the top of the tilt mount as shown in Figure 20 below.

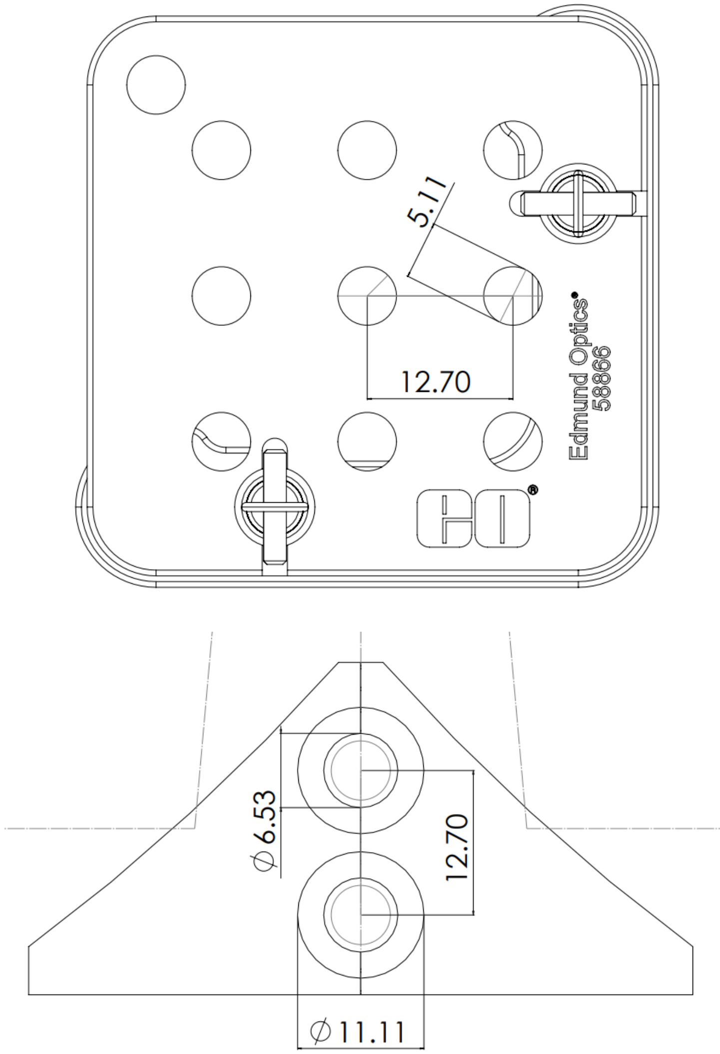

Figure 20. The mounting surfaces of both the tilt mount and the mirror block

Using *Table 5* below, we can determine that the weight of the mirror block and the tilt mount to be 0.285 lbf. This amount of weight is small enough to be considered trivial regarding deciding what post to put them on.

Table 5. Weight Table

Items	Weight(lbf)
Mirrors Block	0.16 +/- 0.01
Tilt Mount	0.125 +/- 0.0022
Source	7.00 +/- 1
Detector	17.00 +/- 3
Cryostat	20.00 +/- 3

4.5 Logistical factors

4.5.1 Budget

The budget is shown below in Table 6.

Table 6. Budget

Item	Cost ($)
Travel	$8553.40
Elliptical Off-Axis Mirror block	$560.00
Tilt Mount	$128.00
Sanding and Polishing	$30.00
Shipping	$40.00
Total cost	$9,311.40
Current Funds	$14303.00

Travel, in this case, will cover flights to and from California, room and board for the duration of the stay there, and expenses such as meals incurred during the visit. This is for both seniors listed at the beginning of this report, their senior design faculty advisor, as well as four other students involved in this project. The five hundred forty dollars estimate for the mirror included machine hours, hourly pay for a student, and the material costs. The tilt mount however can simply be bought stock from Edmund optics ([18]). This fortunately leaves the project in the green.

4.5.2 Schedule

The Schedule is shown below in Table 7.

Table 7. Schedule

Item	Date	Notes
Determine customer needs	N/A	Already acquired from JPL
Library Instruction	1/30	
First draft of Senior Design Proposal	2/17	
Project requirements	2/23	
Final Senior Design Proposal	2/24	
Three Concepts	N/A	
Senior Design Proposal Oral Presentation	3/13	
Experimental design	3/20	
Preliminary Design Review Oral Presentation	4/10	
Optical design	4/21	
Optics Manufactured	5/20	5-week lead time
Pre-Senior Design Report due	4/27	
Experiment at JPL	6/10-6/16	
Analysis	8/15-9/11	
Arrange Weekly Meetings with Senior Design Faculty Adviser	8/21	
Critical Design Review	9/21	
Finalize Analysis of data if Critical Design Review is successful	9/22	
Senior Design Presentation Reviews complete	11/10	
Draft Senior Design Report due to Adviser	11/15	
Final Senior Design Presentation	12/1	
Senior Design Poster Session	12/7	
Final Senior Design Report, due to adviser, shared drive	12/8	
Final Senior Design Report submitted to SOAR	12/15	
Results Presented to JPL	9/22	

This section will include some notes for this schedule. The optics had to be manufactured and not ordered as while the companies we talked to were willing to cooperate with our group, the companies were either within budget and couldn’t fit within our tight schedule, or they could work with our schedule but were out of budget. The schedule for the trip to JPL has been decided. Finally, there will be no hardware ordered next semester as the experiment will be already conducted, any dates related to hardware next semester have been changed to reflect this.

5. Setup and conduct of the Experiment

5.1 Setup of experiment

Upon our arrival at the laboratory, we were introduced to various components that we would be working with. We immediately began setting up and preparing these components. Over the course of the week at JPL, we conducted several sweeps and characterization tests as a build-up to the final experiment, which aimed to determine amplification. Initially, we began by measuring the power output of the FMC, as shown in Figure 10, using an Erickson power meter (PM5) depicted in Figure 22.

Figure 21. Erickson Power Meter

To conduct the PM5 test, we positioned the THz source directly in front of the PM5 detector and measured the output power (absolute power). Additionally, we tested the bolometer and made sure it and the FMC were in the same horizontal plane by placing the bolometer in series with the chopper motor and the FMC, as depicted in Figure 22. The bolometer was responsible for detecting the relative power of the THz source in this setup.

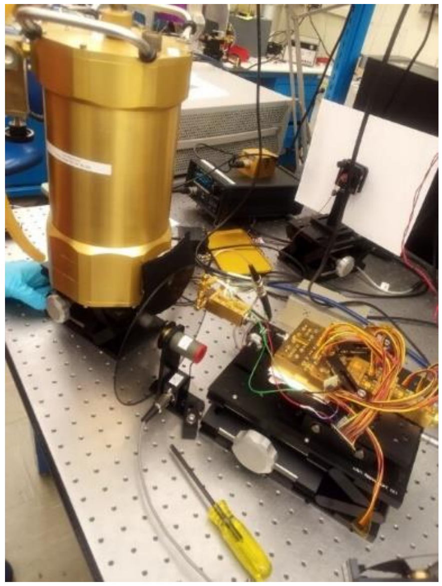

Figure 22. The bolometer (left), the chopper motor (middle), and the FMC (right) placed in series

After testing the bolometer and aligning it to the same horizontal plane as the FMC, it was taken off the stand it was resting on and a red laser put in its place, this red laser can be seen in Figure 23 in the green box. We also placed a mirror over the feed horn of the FMC as can be seen in the left most red box as shown in Figure 23. Finally, we placed a dotted mirror in the place where the metasurface will be located in future steps in order to determine the beam size of a laser and confirm the magnification of the elliptical mirror. This dotted mirror is shown in Figure 23 in the right-most red box.

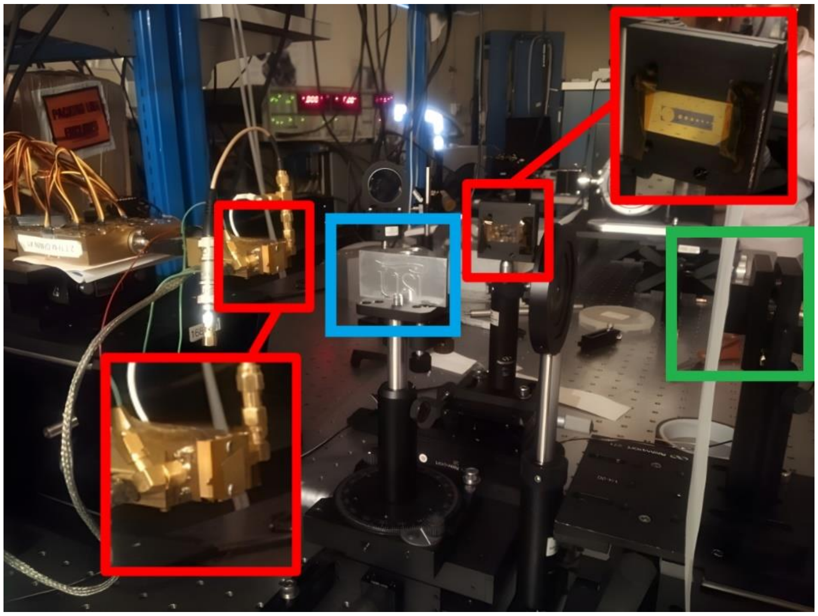

Figure 23. The alignment of the components. The FMC with the covered feed horn (Red Squares to the left), the mirror block (Blue Square in the Middle), the spotted mirror (the red squares to the right), and the red laser (the green laser to the right)

We used the red laser to align the components, visualize the beam path, which is something we cannot do with a THz source because it operates outside of the visible light spectrum, and verify the spot size. First, we adjusted the components until the beam path aligned with the arrows depicted in (1) in Appendix F and (2) in Appendix F. Second, we verified the beam size and magnification of the mirror by comparing it to the size of the dots on the dotted mirror. We then replaced the dotted mirror with the Stirling Cooler housing the QCMSA as shown in Figure 24. and aligned it using the red laser.

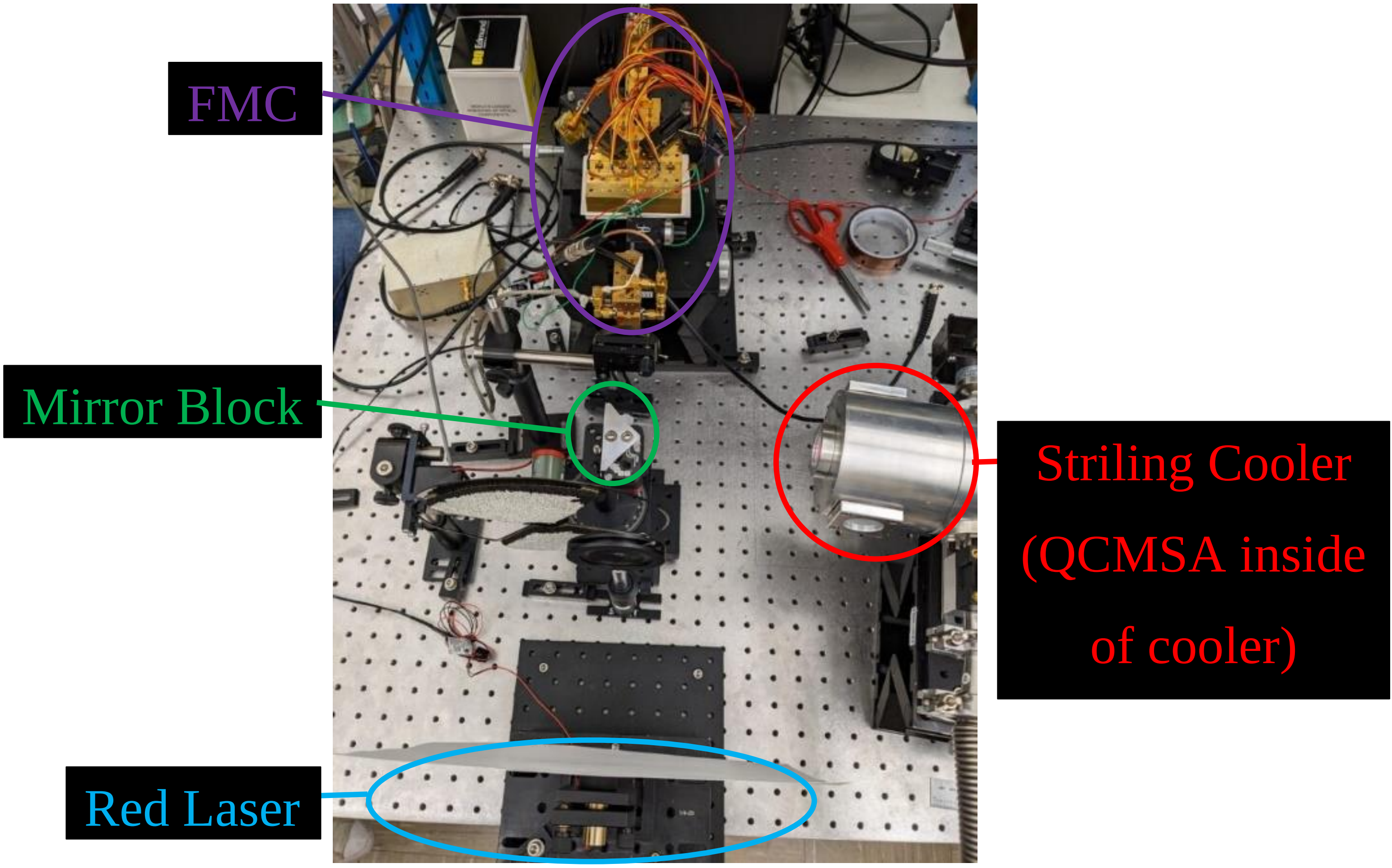

Figure 24. Testbed after dotted mirror was replaced with the Stirling cooler housing the QCMSA.

The alignment of the QCMSA was done similarly to the process depicted in Appendix F and described above. We could do this because the metasurface behaves like a flat mirror in optical light. After the alignment was complete, we replaced the red laser with the detector, a silicon bolometer operating at 4 K. The collecting area of the bolometer is large relative to the incoming THz beam size, so the bolometer did not need as precise of alignment. The final testbed setup can be seen in Figure 25.

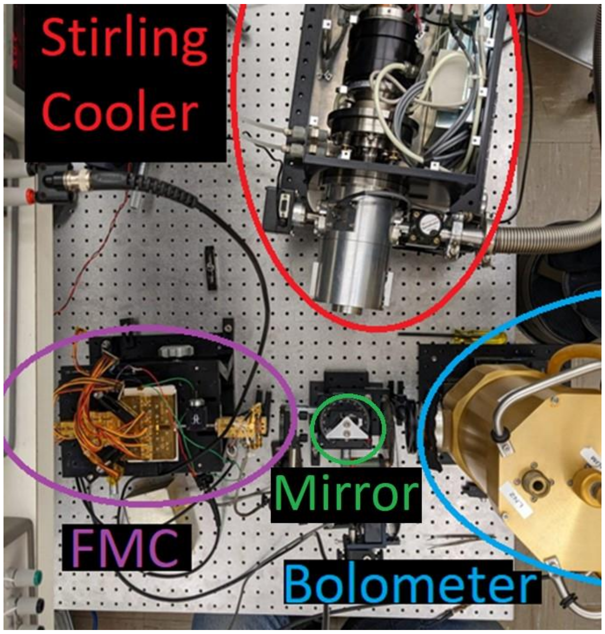

Figure 25. The final setup of the testbed used to to test the amplification of a QCMSA

After the testbed was fully assembled, we turned on the FMC and bolometer, and adjusted the metasurface back and forth to minimize the spot size with the THz beam. Because light at THz frequency cannot be seen with the human eye, we used knife edge measurements to determine the spot size on the meta surface. These knife edge measurements, shown in Figure 26, were done by slowly sliding a piece of paper in towards the edge of the metasurface and watching for the power read out from the bolometer to attenuate. When the power drops, we know that the paper has reached one edge of the beam. We would then do the same procedure to find the opposite edge of the beam and take the difference between both edges to determine the diameter of the beam.

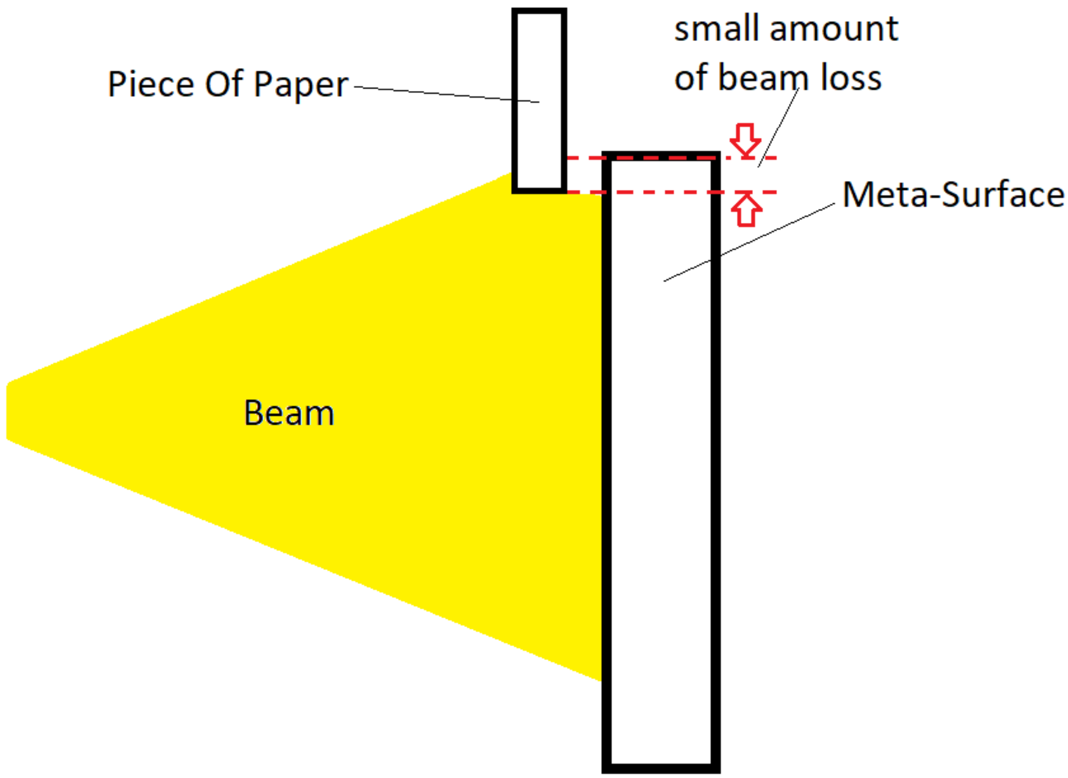

Figure 26. Knife edge measurement to determine the size of the THz beam at the metasurface. A piece of paper is slowly inserted until the power of the THz beam begins to attenuate. This is done for both sides of the beam and the distance between the two sides determines the beam diameter.

5.2 Conduct of the experiment

After measuring the output power of both the PM5 and bolometer, we concluded the bolometer was more sensitive and used it to collect our data. We collected data by conducting frequency sweeps, a procedure that entails increasing the frequency coming out of the FMC by increments of 0.005 THz between 2.45 THz and 2.75 THz using a frequency synthesizer shown in Figure 27 and recording the voltage displayed on a lock-in amplifier at each increment. The beam path for these frequency sweeps is shown in Figure 28.We conducted frequency sweeps with the bolometer while varying the temperature of the cryostat, both warm and cold. These frequency sweeps helped us analyze and understand the behavior of our components. It is preferable to remove as much heat as possible from the cryostat because this results in reduced performance degradation. In simpler terms, when comparing the warm and cold sweeps, the power output should be higher in the cold cryostat, indicating improved performance. After this we conducted three frequency sweeps with three different voltage biases applied to the QCMSA, one with no voltage bias, one with a 3-volt bias, and one with a 5-volt bias, all conducted with the QCMSA cryostat at 50° K.

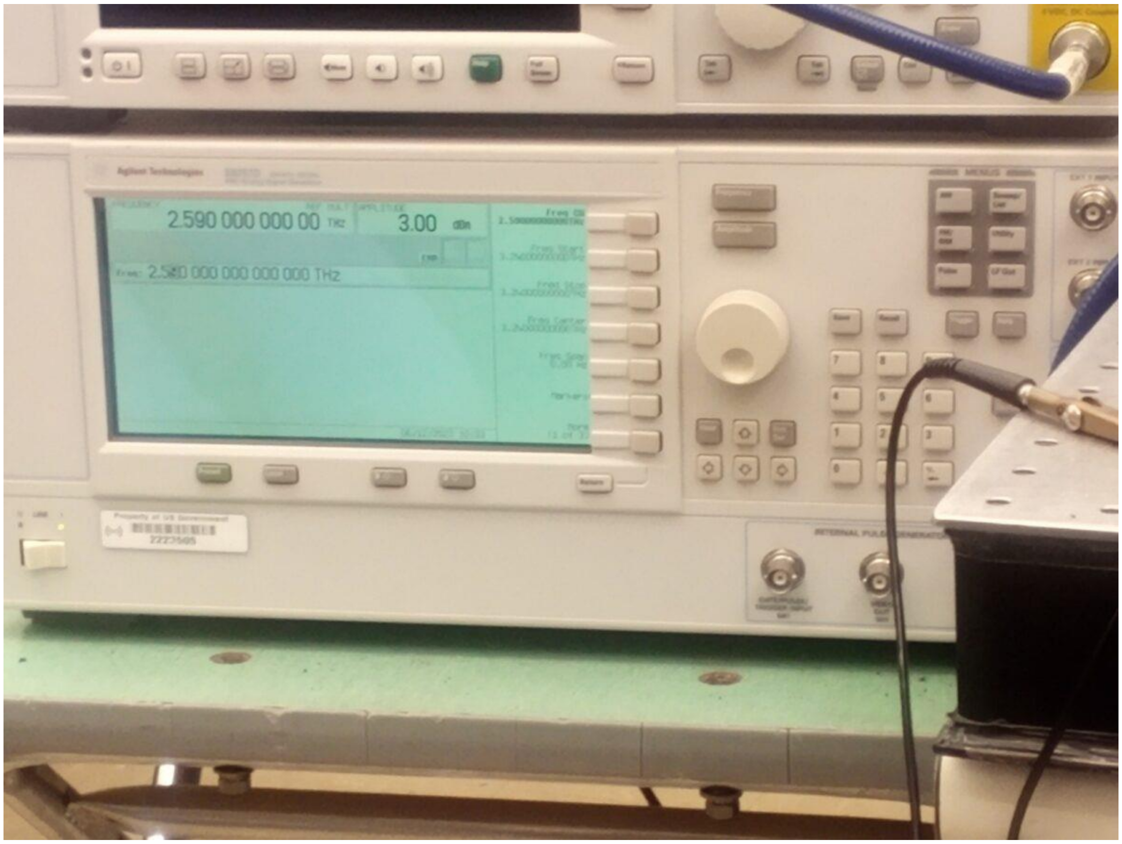

Figure 27. Frequency Synthesizer

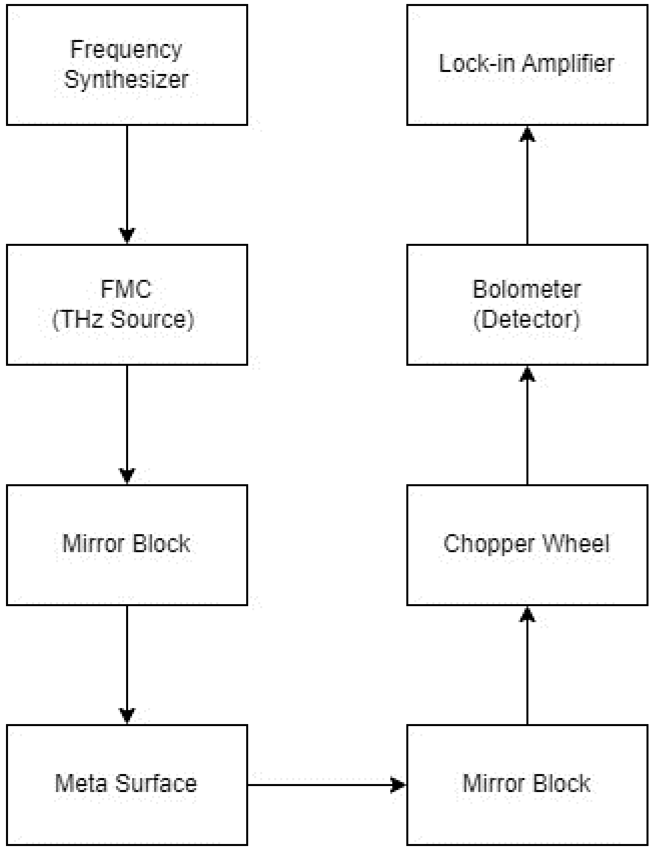

Figure 28. Beam Path for Data Collection

6. Results of the Experiment

6.1 Relative Power with PM5 vs. Bolometer

The Erickson power meter (PM5) was initially used to measure absolute power, but due to its lower sensitivity compared to the bolometer, we swiftly transitioned to using the bolometer for the remaining tests. A comparison of Figure 29 and Figure 30 reveals that the bolometer detected significantly higher power, this was due to the bolometer being more sensitive and having a finer resolution and thus a more accurate gain. The bolometer was able to reach a higher sensitivity due to it detecting the difference in power with the chopper motor cutting the frequency. It is worth noting that both figures involved positioning the FMC source directly in front of the detectors to measure power. This approach was taken to facilitate a comparison between the detectors and affirm that the higher power in the bolometer was just a scaling factor.

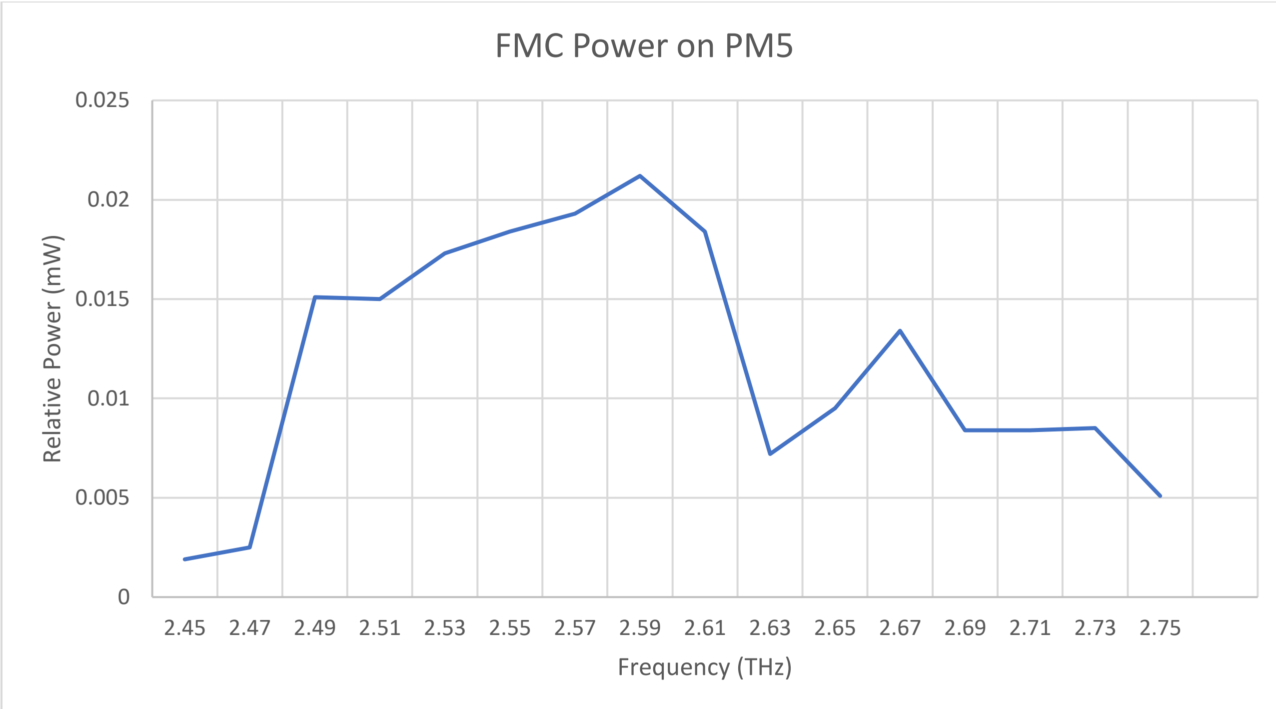

Figure 29. Erickson power meter FMC relative power vs. frequency

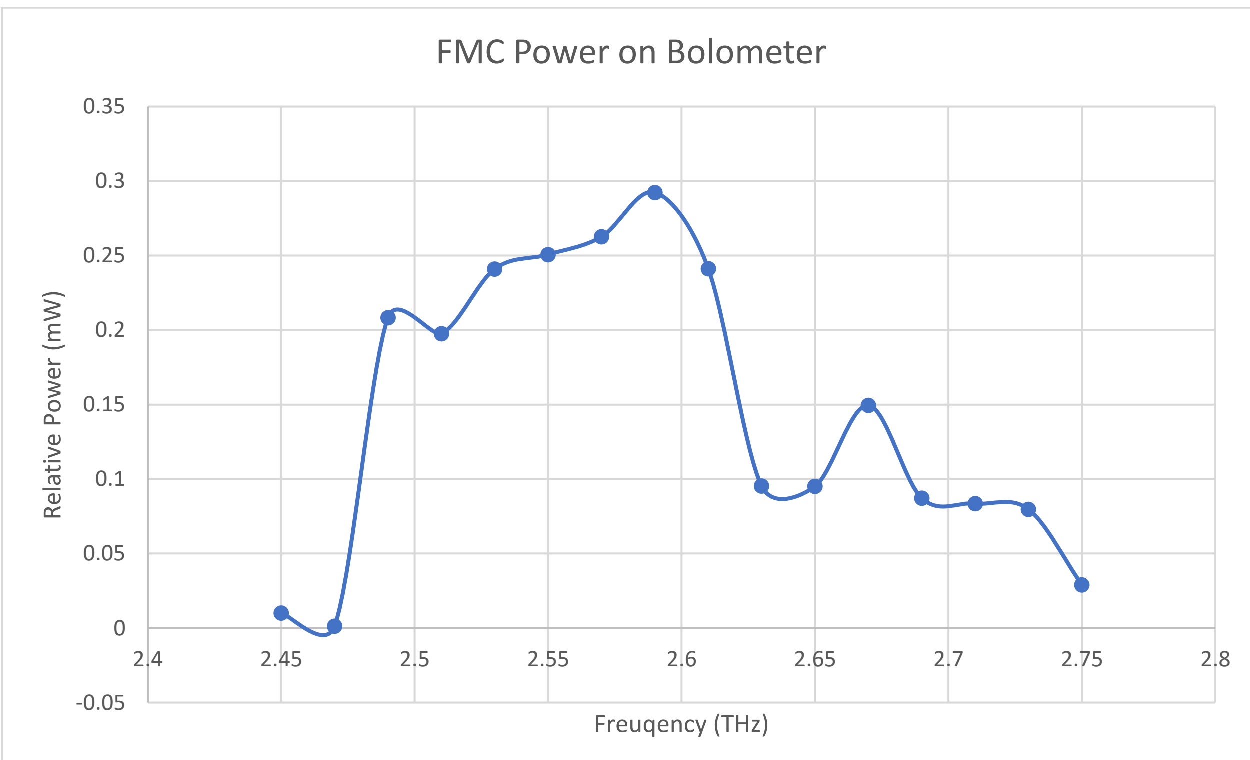

Figure 30. Bolometer FMC relative power vs. frequency

The bolometer records relative power, which is measured using a lock-in amplifier synchronized with the chopper motor's frequency. This amplifier then computes the power difference between the background and THz beam as the chopper wheel modulates the signal between an on and off position. This computed disparity in power represents the relative power recorded for the data.

6.2 Frequency sweeps for gain demonstration

The frequency sweeps encompassed a range of bias voltages: 3V, 5V, and 0V. The 0V bias was denoted as the reference frequency sweep, while the 3V and 5V biases involved applying these voltages to the metasurface and conducting the frequency sweeps as detailed earlier. To demonstrate whether we had gain, we collected data from both the 3V and 5V bias sweeps and compared both to the reference frequency sweep. To visually compare these sweeps, we converted the power ratio between the 5V and 0V sweep and the 3V and 0V sweep to a decibel scale by applying a logarithm (base 10) to both ratios, and then multiplying by 10 to create a plot of gain vs. frequency shown below in Figure 31.

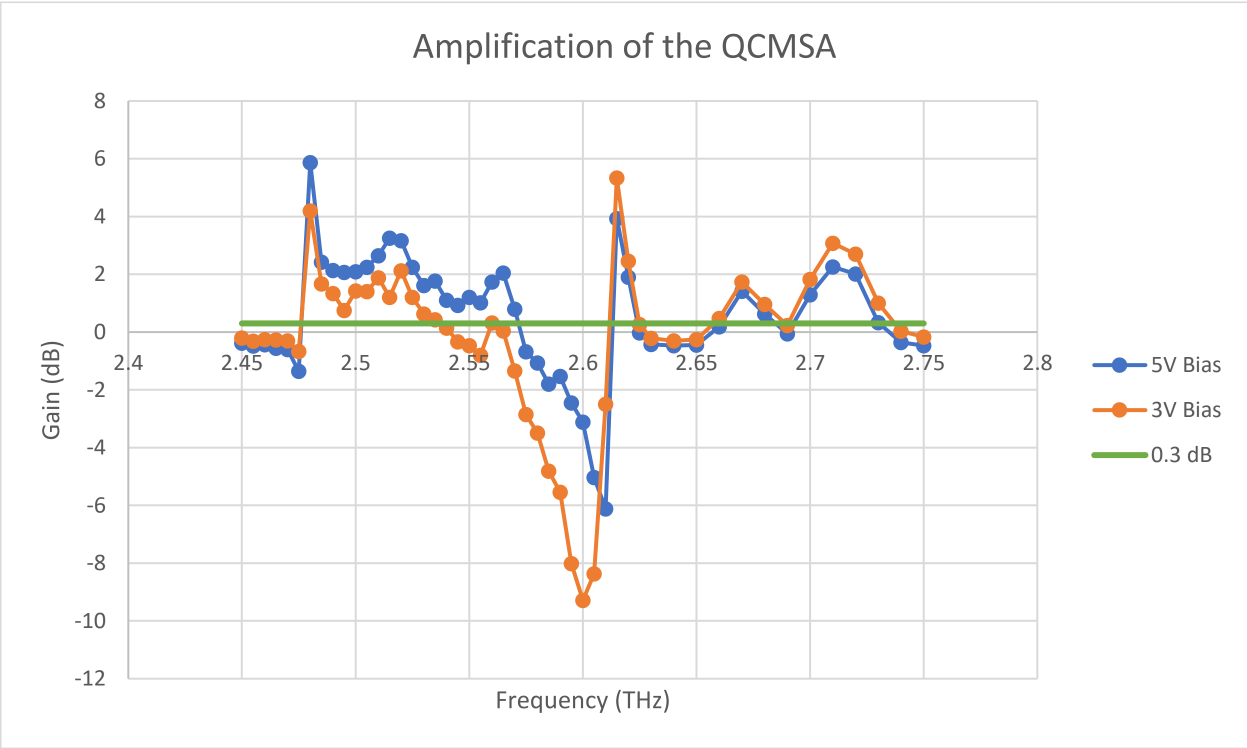

Figure 31. Plot of gain vs. frequency

The results show most of the recorded amplifications were over the required 0.3 decibels.

Between the frequencies of 2.554 and 2.62 there is dip in amplification, which is caused by THz radiation being absorbed by water molecules in the atmosphere. When THz radiation (light) interacts with water molecules, certain frequencies associated with rotational and vibrational energy transitions are absorbed, which leads to a dip in the detected signal. We found the 5V bias had more amplification to the left of the water line and on the water line, as depicted in Figure 32. The 3V bias had more amplification to the right of the water line, as depicted in Figure 33. Overall, however, the 5V bias had a stronger response across the board.

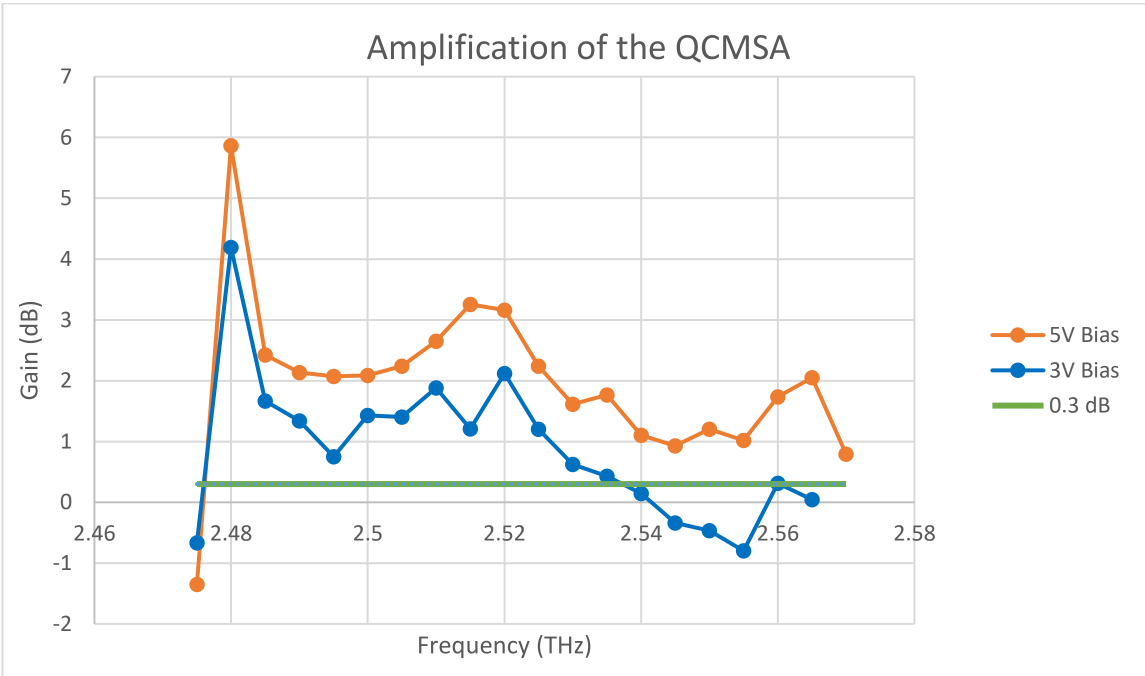

Figure 32. Plot of Gain vs. Frequency to the Left of the Water Line

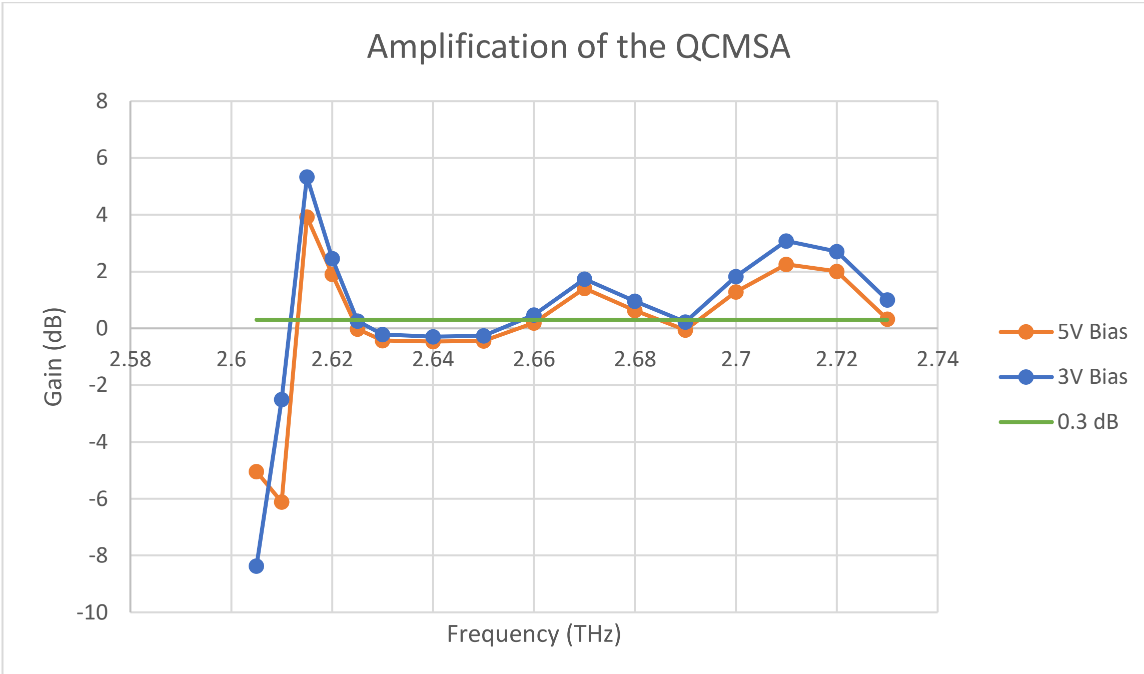

Figure 33. Plot of Gain vs. Frequency to the Right of the Water Line

6.3 Spot size on meta surface

Although the amplification surpasses the 0.3 dB requirement, the spot size did not meet the 1 mm requirement. As seen in Table 8, the minimum beam diameter we measured at the QCMSA using the knife edge technique was 1.27 mm. There were attempts to adjust the distances of both the metasurface and the FMC, but, as shown on Table 8, any adjustments made resulted in an increase in beam diameter at the QCMSA.

Table 8. Spot Size Adjustments

FMC Adjustments		
Distance (mm)	Spot Size of Beam (in)	Spot Size of Beam Diameter (mm)
-30	0.056	1.4224
0	**0.05**	**1.27**
30	0.064	1.6256
Flat Mirror Adjustments		
Distance (mm)	Spot Size of Beam (in)	Spot Size of Beam Diameter (mm)
-10	0.06	1.524
0	**0.05**	**1.27**
10	0.1	2.54

This result could have happened for a few different reasons, there could have been a miscommunication with JPL about the feedhorn size which would have changed our beam size at the mirror, see Equation (7). Additionally, there could have been small misalignments between the components and, with optics especially, that can provide an ample source of error. There is also a possibility that there could have been defects with the manufacture of the mirror block or a change in shape of the mirror block during the sanding and polishing process. Finally, the power drop we saw could have been us attenuating a side lobe. Side lobes, shown in Figure 34. Side lobes and main lobe coming from feed horn., are energy transmitted outside of the main beam of light and are a common side effect in antenna. In this case these sidelobes were a result of diffraction caused by the feed horn.

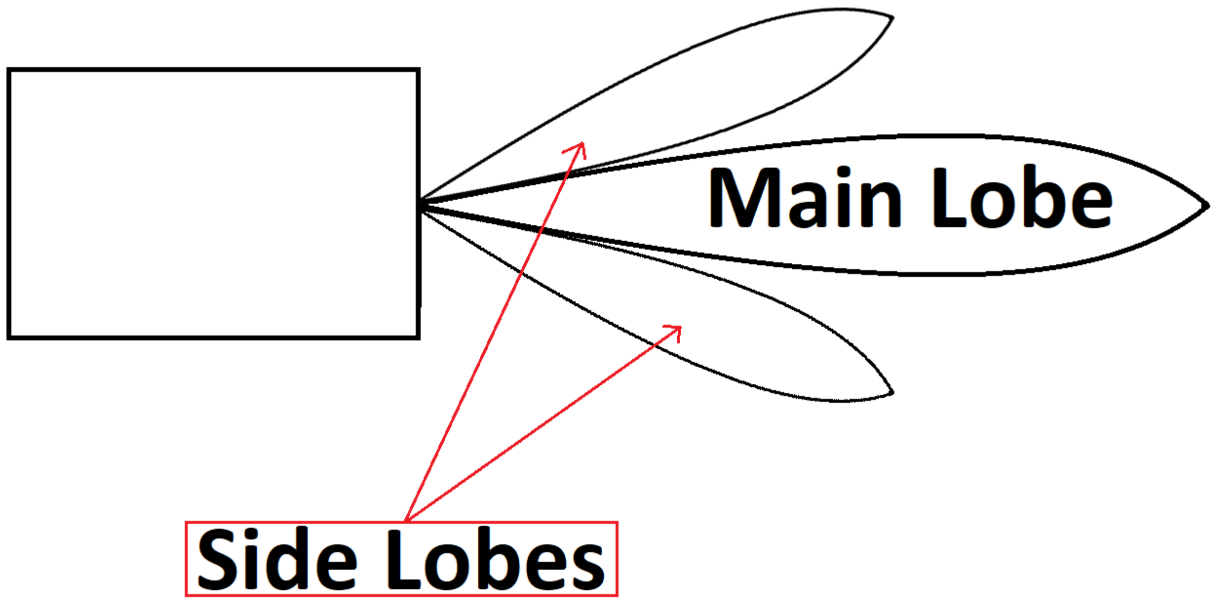

Figure 34. Side lobes and main lobe coming from feed horn.

7. Conclusion

7.1 Lessons Learned

The development of optics, the designing of the optical testbed, and using the optical testbed for research provided much useful information. The team learned about the usefulness of pre-project research analysis sessions. Before the project began, our group would gather on campus weekly, in these meetings, team members reviewed relevant research papers to gain a comprehensive understanding of the current state of knowledge in the project's subject area. These discussions helped the team identify gaps and opportunities, shaped the project's direction, and ensured that their work was built upon a solid foundation of existing research. The team gained useful knowledge in the field of optics and useful information about the manufacturing of optics. Additionally, the team acquired knowledge on the procedures for conducting experiments and gained insights into the methods for analyzing recorded data.

7.2 Final Remarks

The overall goal of this project was to create an optical testbed to measure the QCMSA's amplification abilities. During the development of the testbed, the requirements given to us by JPL changed multiple times. Fortunately, the choice to use the python script shown in Appendix E proved invaluable as it allowed for the equations and variables to be quickly changed, the dimensions for the mirror and the spacing for the testbed to be quickly found, and for all of the new data to be quickly re-tested to ensure functionality. Ultimately, the team developed a design that aligned with the testbed's requirements and a mirror design that satisfied all but one of the specified criteria in Table 1. The unmet requirement pertained to the spot size. Nonetheless, the experiment yielded amplification, suggesting potential for significantly greater amplification estimated at 10-20 dB if the spot size meets specifications. It is recommended to explore a similar experiment using a Quantum Cascade Laser (QCL) as an alternative to the FMC.

References

[1] National Science Foundation. *Master Government List of Federally Funded R&D Centers*. February 2023. webpage. 12 April 2023.

[2] Walker, Christopher K. *Terahertz Astronomy*. CRC Press, 2019.

[3] Seo, Young Min, et al. *Probing ISM Structure in Trumpler 14 & Carina I Using The Stratospheric Terahertz Observatory 2*. 2019.

[4] Hollenbach, D. J., and A. G. G. M. Tielens. "DENSE PHOTODISSOCIATION REGIONS (PDRs)." *Annual Review of Astronomy & Astrophysics. 1997, Vol. 35 Issue 1, p179. 37p.* 1997: p179. 37p.

[5] Sarkar, Tapan K. "Heterodyne Detector for Wireless Telegraphy." *History of Wireless,Wiley, Hoboken, NJ,* 2006: pp. 370–372. Wiley Series in Microwave and Optical Engineering.

[6] Howell, J. Q. "Microstrip antenna." *IEEE Transactions on Antennas and Propagation* vol. AP-23 1975: pp. 90–93.

[7] Pakfetrat, Faezeh, and Hassan Pakarzadeh. "Terahertz Plasmonic Quantum Cascade Lasers: A Comprehensive Physics Study." *Plasmonics* vol. 17, no. 3 2022: pp. 913–20.

[8] Williams, Benjamin S.(Benjamin Stanford). *Terahertz Quantum Cascade Lasers*. Thesis. Cambridge: Massachusetts Institute of Technology, 2003.

[9] Christopher A. Curwen, et al. "ment of Amplification and Absorption of a THz Quantum-Cascade Metasurface Free-Space Amplifier." *AIP Advances* vol. 12, no. 11 2022.

[10] Hirokatsu Yumoto, et al. "X-Ray Microfocusing with off-Axis Ellipsoidal Mirror." *AIP Conference Proceedings* , vol. 1741, no. 1 2016: pp. 1–4. EBSCOhost.

[11] Ren, Y., et al. "Single Mode Terahertz Quantum Cascade Amplifier." *Applied Physics Letters* vol. 105, no. 14 2014: pp. 1–4.

[12] Salimi, Tohid, et al. "Design of a Compact Gaussian Profiled Corrugated Horn Antenna for Low Sidelobe-Level Applications." *International Journal of Computer Theory and Engineering* vol. 5, no. 2 2013: pp. 223–226.

[13] Goldsmith, Paul F. *Quasioptical Systems: Gaussian Beam Quasioptical Propogation and Applications. 1st ed*. Wiley-IEEE Press, 1998.

[14] Selstad, Johnathon. “Ellipsoidal Mirrors.” Sublucid Geometry, 18 Jan. 2020, https://zalo.github.io/blog/ellipsoids/. n.d.

[15] “Off-Axis Ellipsoidal Mirrors: Edmund Optics.” Edmund Optics Worldwide, https://www.edmundoptics.com/f/off-axis-ellipsoidal-mirrors/39583/. n.d.
[16] “Development of an Ellipse from the Definition.” Development of an Ellipse from the Defintion, https://people.richland.edu/james/lecture/m116/conics/elldef.html. n.d.
[17] Sparknotes, SparkNotes, https://www.sparknotes.com/math/precalc/conicsections/section3/#:~:text=The%20standard%20equation%20of%20an,%3D%20a2%20%2D%20b2. n.d.
[18] https://www.edmundoptics.com/f/kinematic-table-platforms/13287/
[19] https://www.acesolution.com.tw/tw/products/product_VDI_PM4.html

Appendices

Appendix A

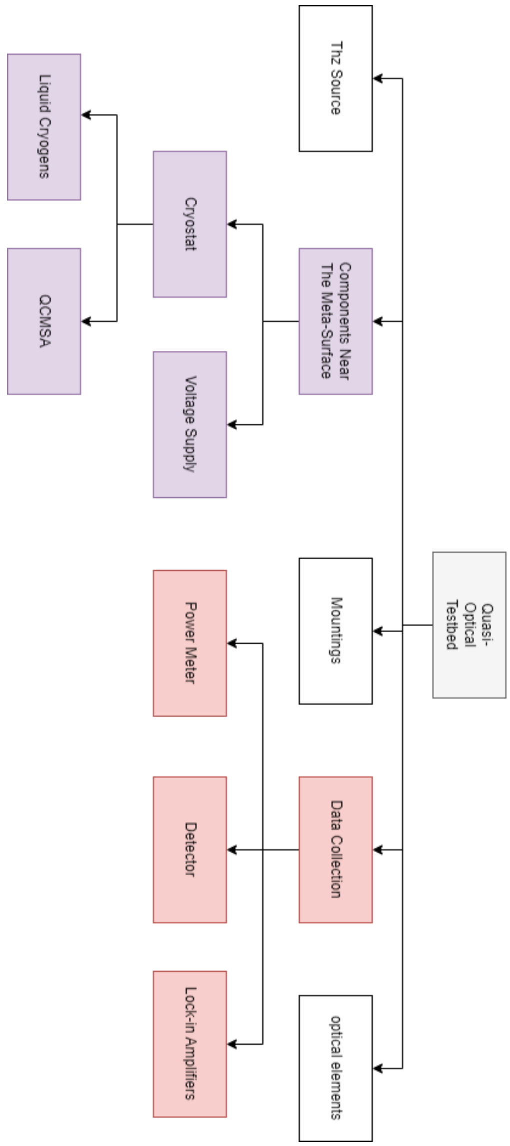

Figure 35. System Hierarchy

Appendix B

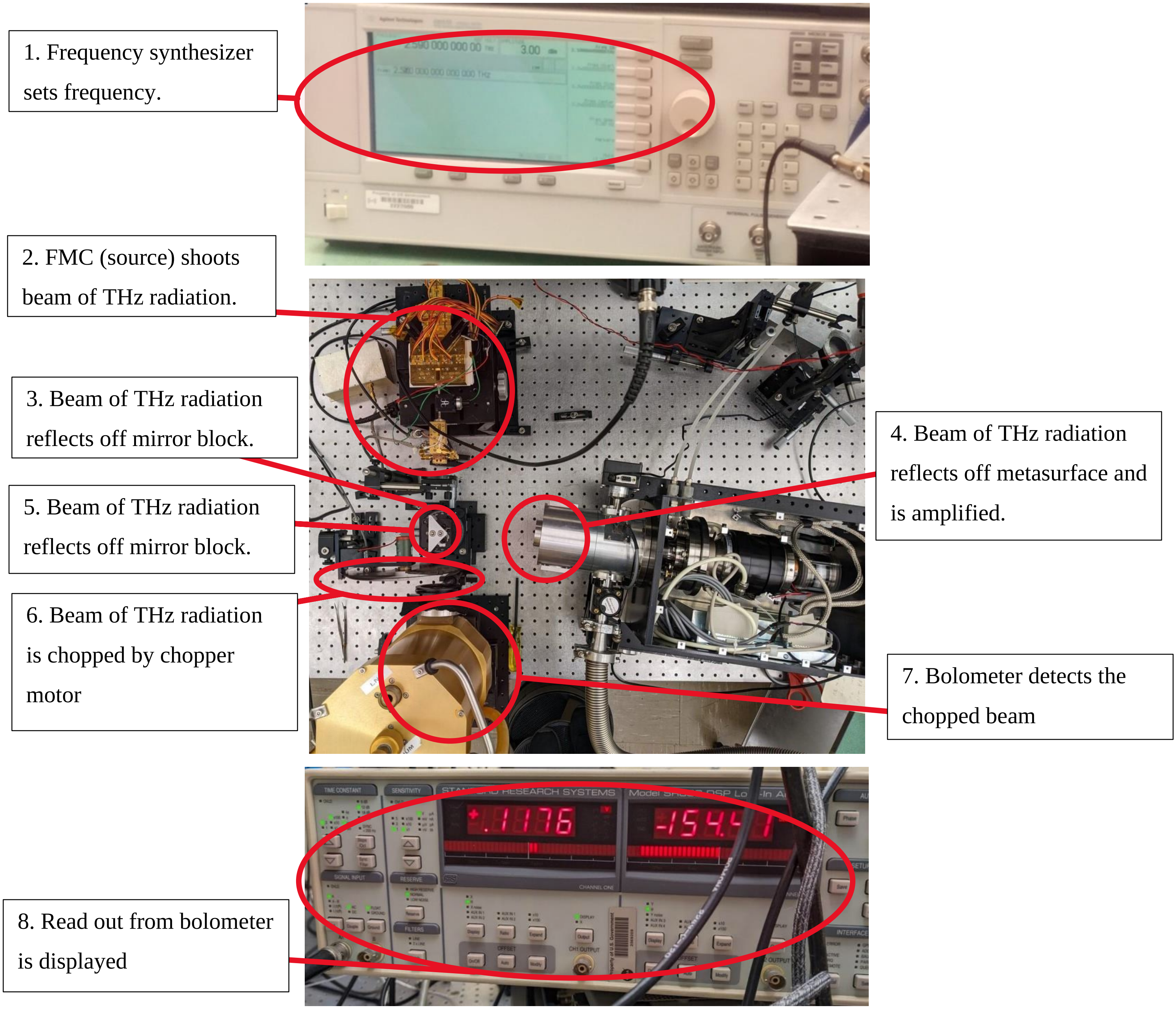

Figure 36. Concept of operations

Appendix C

Table 9. Failure Mode Analysis for Before we get to JPL

Item	Failure Modes	Cause of Failure	Possible Effects	Probability	Level	Possible action to reduce failure rate or effects
Mirrors	Broken or scratched	-Damage during delivery -Poor production -Defective materials	Beam interference	Medium	Critical	-Order early on to allow for re-order
Electronics	Burnout	-Poor delivery or production	Test bed not functional	low	Critical	-Make sure backup parts are available
Electronics	Defective	-Improperly produced/delivered	Test bed not functional	Low	Critical	-Make sure backup parts are available or order early on to allow for re-order
Quantum cascade meta-surface	Defective	-Improperly produced/delivered	Test bed not functional	Low	Critical	-Order early on to allow for re-order
Optical-testbed	JPL does not have prepare the needed parts	-Design document poorly describes needed components	Not able to construct the test bed	Medium	Critical	-Have design reviewed by a third party and ask what they think is necessary to order to test the descriptiveness of the design -Have design reviewed by faculty advisor - Have design reviewed by every team member

Table 10. Failure Mode Analysis for After we get to JPL

Item	Failure Modes	Cause of Failure	Possible Effects	Probability	Level	Possible action to reduce failure rate or effects
Mirrors	Broken or scratched	-Mishandling	Beam interference	Medium	Critical	-Develop procedures for handling the optics
Electronics	Burnout	-Mistake in wiring setup -Liquids being spilled on wiring	Test bed not functional	High	Critical	-Double Check Wiring setup -Disallow any liquids in room with test bed

Appendix D

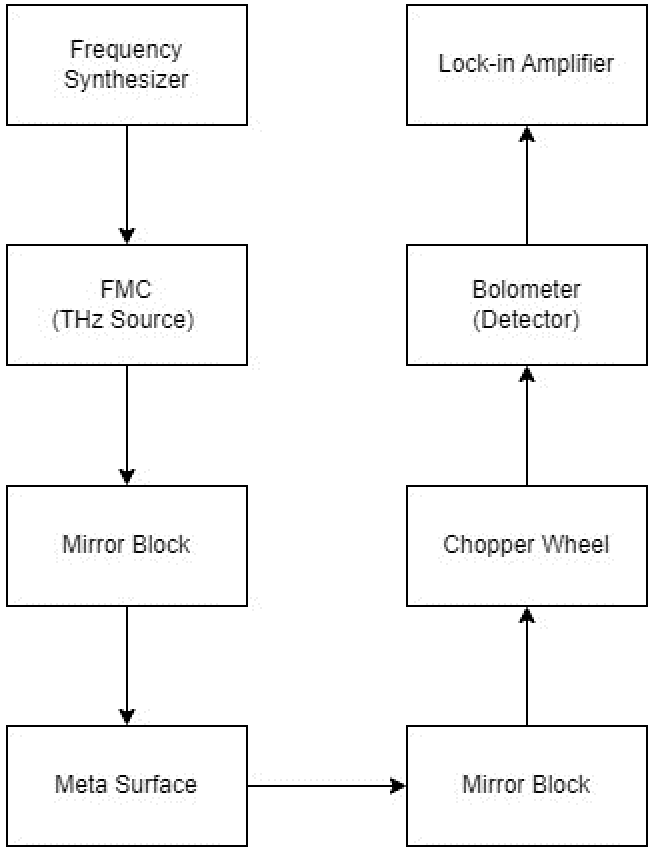

Figure 37. Functional block diagram

Appendix E

```python
'''for the more than 90 degrees ellipsodial mirror
focused on theta reduction'''
'''Kassidon Hatfield'''
import math
import pandas as pd
f1=100
mag=1.65
offSet=95
f2=mag*f1
h=((f2**2)+(f1**2)-(2*f1*f2*math.cos(offSet*(math.pi/180))))**(1/2)
a=((f1+f2)/2)
b=(a**2-(h/2)**2)**(1/2)
print('h: '+str(h)+
      ' mm\nf1: '+str(f1)+
      ' mm\nf2: '+str(f2)+
      ' mm\nMagnification: '+str(f2/f1)+
      '\na: '+str(a)+
      ' mm\nTail: '+str(((a)-(h/2)))+
      ' mm\nb: '+str(b)+' mm'
)

RadtoDeg=180/math.pi
fr=2.7*(10**12)
Lamduh=0.0001110342
f1=f1/1000
f2=f2/1000
MetaSurfacePlacement=0.005
WOin=.242/1000
WOout=(f2/f1)*WOin
z1=f1
z2=f2
DmRanger=2
Wz=((WOin**2)*(1+((Lamduh*z1)/(math.pi*(WOin**2)))**2))**(1/2)
Dm=DmRanger*Wz
z2=z1*(WOout/WOin)
Wwindow=(((WOout**2)*(1+((Lamduh*MetaSurfacePlacement)/(math.pi*(WOout**2)))**2))**(1/2))
Theta=(math.asin((Dm)/((2*z2))))*RadtoDeg
mirrorclearance=((math.sin((Theta)*(math.pi/180)))*(f2))
print('z1 = '+str(z1*1000)+
      ' mm \ndiameter of mirror: '+str(Dm*1000)+
      ' mm \nTheta: '+str(Theta)+
      '\nWz: '+str(Wz*1000)+
      ' mm'+'\nBeam Diameter at Window: '+str(Wwindow*1000*2)+
      ' mm'+'\nWOin: '+str(WOin*1000)+
      ' mm'+'\nBeamDiameterAtSurface: '+str(2*WOout*1000)+' mm' )

print((mirrorclearance-(Dm/2))*1000)
```

Figure 38. Python script used for calculations

Appendix F

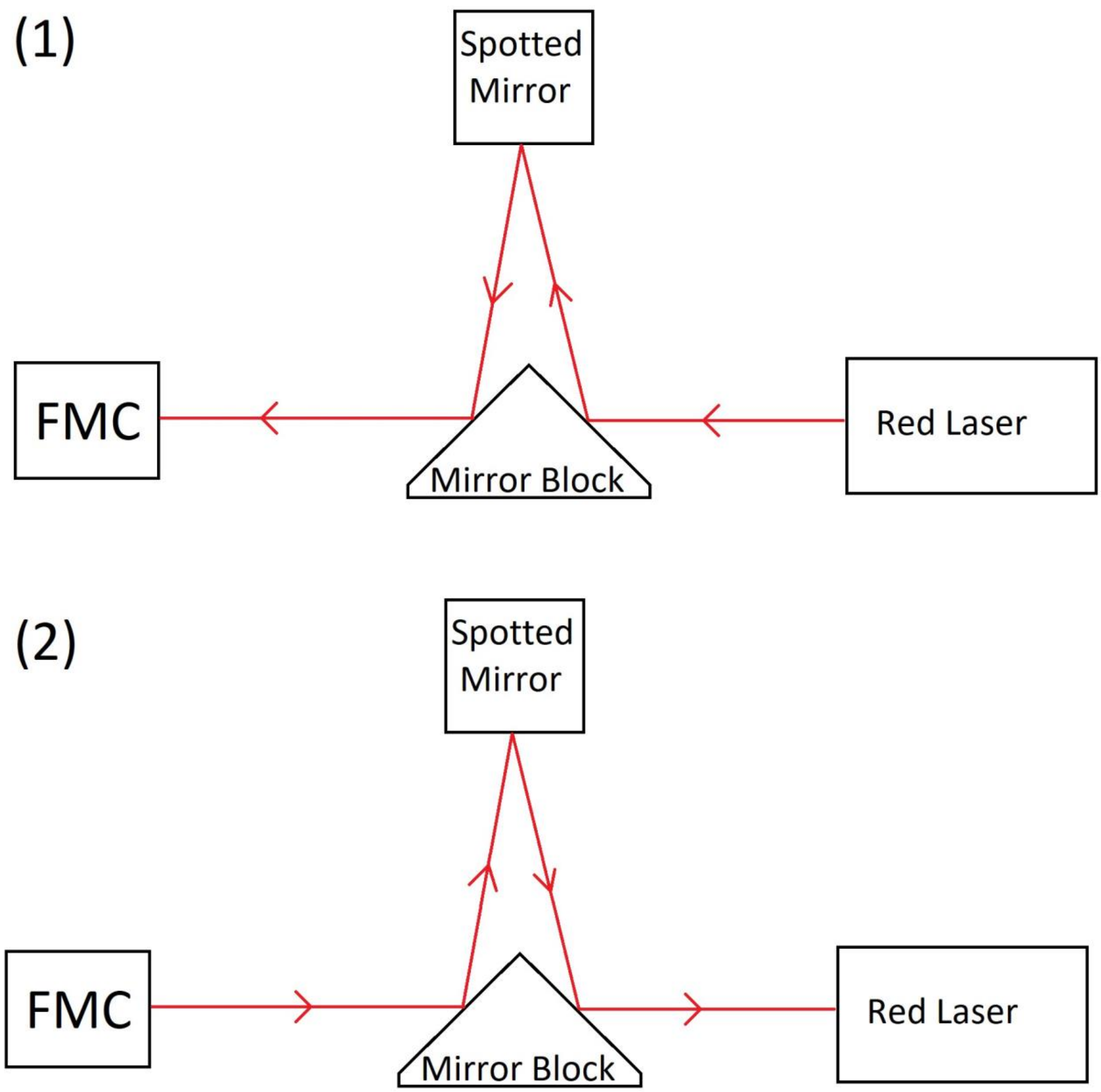

Figure 39.Beam Path During alignment. (1) depicts the beam path after it exits red the laser and before it reaches the FMC. (2) depicts the path after bounces off the mirror placed on the FMC and returns to the red laser.

Appendix G

Table 11. Impacts of Project

Design Factor	Impacts
Public Health, Safety, and Welfare	This amplifier could be used for military purposes. The amplifier could be used and would be targeted to heat water or unzip DNA. Therefore, this could be used as a crowd control or in some other ways that benefit the military.
Global	This experiment will impact the way international scientists in Europe and Asia will design THz heterodyne receivers.
Cultural	Brought together students from a rural University (USI) and scientists from the second largest metro area in the US to take measurements of the amplifier.
Social	Does not have a social impact.
Economic	Will enable JPL and the advisor of the project to apply for NASA funding to fly a balloon with this technology to look at star formation in the Milky Way and nearby galaxies.
Environmental	Does not have an environmental impact.
Ethical & Professional	Does not have an ethical & professional impact.